Validation of Heat Transfer Correlations in Line Chill-down Tests of Cryogenic Fluid in SINDA/FLUINT

Barbara Sakowski, Daniel M. Hauser, & Jason W. Hartwig
NASA/Glenn Research Center

M. Kassemi
National Center for Space Exploration Research (NCSER)

Cleveland, OH, 44135, USA

Line Chill-down heat transfer was modelled using SINDA/FLUINT. Multiple chill-down tests were modelled using the heat transfer correlations that are available in SINDA/FLUINT, as well as incorporating heat transfer empiricisms developed by the University of Florida[1] based on a series of liquid nitrogen chill-down tests. The chill-down tests that were modelled were the liquid nitrogen tests conducted by the University of Florida[1] as well as liquid hydrogen tests conducted by NASA Glenn Research Center[2]. The liquid nitrogen tests included horizontal flow, upward flow, and downward flow with the liquid Reynolds Numbers ranging 850 – 231,000. The liquid hydrogen test was vertical upward flow at a Reynolds Number range of 18,400 – 433,000. Both the University of Florida's heat transfer correlations and SINDA/FLUINT's internal correlations faired similarly to wall temperature test data. They were acceptable although improvements could be made to the University of Florida correlations as well and SINDA/FLUINT's internal correlations.

I. Nomenclature

c_p = specific heat at constant pressure, J/(kg·K)
D = inner diameter of tube, m
F = multiplication factor on Dittus Boelter
FR = flow rate, kg/s
G = mass flux, kg /(m^2·s)
g = gravity, m/s^2
h = heat transfer coefficient, W/(m^2·K)
h_{fg} = latent heat, J/kg
Ja = $1/(h_{fg}/ c_{pl}(T_w-T_{sat}))$
k = thermal conductivity, W/(m·K)
L = distance downstream of inlet, m
Nu = Nusselt number, hD/k
Pr = Prandtl number, $C_p\mu/k$
q" = heat flux, W/ m^2
Re = Reynolds number, GD/μ
S = multiplication factor on Dittus Boelter
T = temperature, K
Tw = wall temperature, K
Twet = rewetting temperature, K
Tleid = Leidenfrost temperature, K
Tsat = saturation temperature, K
T_{cr} = critical temperature of the working fluid, K
We = Weber number, $G D^2/ (\rho\sigma_l)$
X = mass quality
Xa = actual quality
Xe = equilibrium quality
μ = dynamic viscosity, Pa·s

ρ = density, kg/m^3
ν = specific volume, m^3/kg
σ = surface tension, N/m

Subscripts

CHF = critical heat flux
D = inner diameter of tube
DB = Dittus-Boelter
dfb = departure of film boiling
f = fluid
fb = film boiling regime
fg = saturation
L = length of tube
l = liquid property at saturation
nb = nucleate boiling regime
sp = single phase
sub = subcooled
tb = transition boiling regime
v = vapor property at saturation
w = wall

II. Introduction

Chill-down is an important process in cryogenic tank propellant management, storage, and usage. The process of chill-down is required to cool hardware so that liquid flow can be delivered to in-space propulsion engines or propellant tanks. Complex flow dynamics during these processes include various types of boiling heat transfer (film, transition, and nucleate boiling). It is important to have the ability to model this phenomena so that efficient line chill-down systems can be built that use less propellant. This results in less propellant stored, thereby reducing cost for space missions.

SINDA/FLUINT (SF) is a multipurpose thermal and fluid analysis code that contains correlations for heat transfer and pressure drop. SINDA/FLUINT (version 5.8) was used to model heat transfer in multiple chill-down tests using the heat transfer correlations that are readily available in the code. Heat transfer empiricisms developed by the University of Florida (UF) were also incorporated through extensive user written logic. These correlations were based on a series of liquid nitrogen chill-down tests. The liquid nitrogen tests included horizontal flow, upward flow, and downward flow spanning a range of Reynolds Numbers from 850-231,000. These tests were numerically modelled as well as a liquid hydrogen vertical upward flow test conducted by NASA Glenn Research Center. These hydrogen chill-down tests spanned a range of Reynolds Numbers from 18,400-433,000.

The wall temperature results using the internal correlations in SINDA/FLUINT were compared to the wall temperature results using the empiricisms developed by the University of Florida, as well as to test data. The results for the liquid nitrogen cases seemed to slightly favor the University of Florida correlations for heat transfer, as compared to test data, over the internal SINDA/FLUINT correlations. However there were some test cases where the SINDA/FLUINT correlations deviated from the test data significantly primarily in the film boiling regime. There were also test cases where the empiricisms from the University of Florida deviated significantly from the test data due to flow rate oscillations in the entrance section of the pipe. These flow rate oscillations did not affect the SINDA/FLUINT correlations. In the liquid hydrogen test cases, both the University of Florida's empiricisms and SINDA/FLUINT's correlations faired about the same relative to the test data. Both generated acceptable comparisons to test data albeit not as good as the comparison to the liquid nitrogen test data

It should be noted that the models for both chill-down systems created in SINDA/FLUINT only represented a portion of the test section. Details of upstream and downstream flow dynamics were not modelled. Boundary conditions for the models used the flow rate measured in the system along with pressure measured upstream of the test section. Attempts to model either system using only pressures at the upstream and downstream of the test section resulted in excessive flow rates that did not correspond to the test data flow rate or comparable wall temperatures to the test data. The excessive flow rates caused large heat transfer coefficients to be calculated, thereby too rapid of a wall chill-down.

III. Liquid Nitrogen Chill-down Model

A schematic of the liquid nitrogen chill-down test is shown in Figure 1.

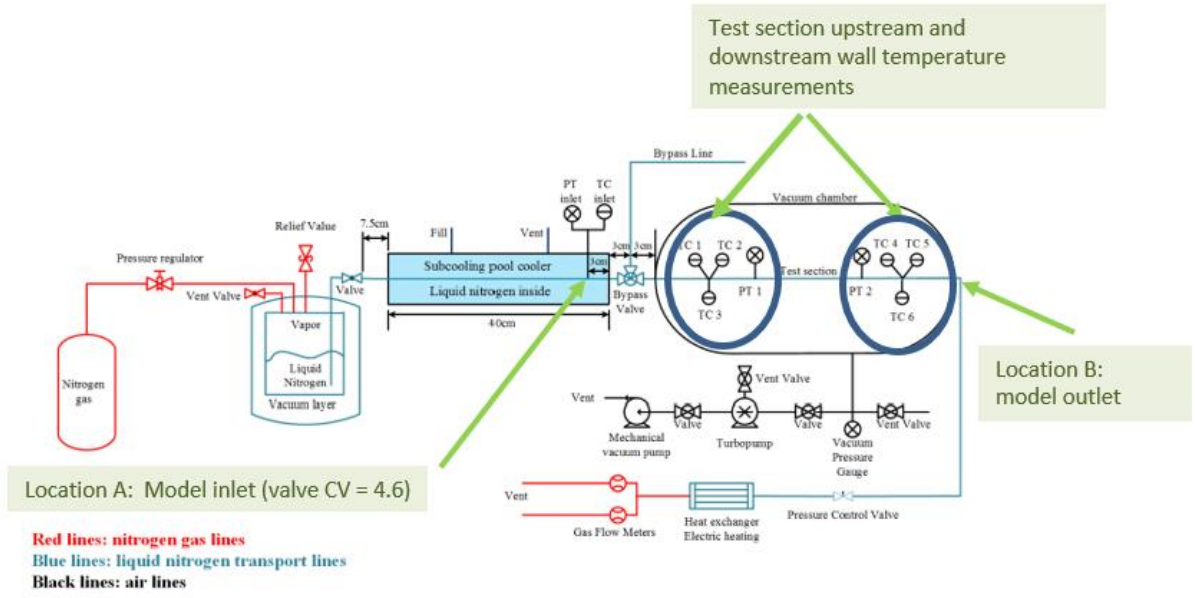

Figure 1: Liquid Nitrogen Chill-down Test Schematic

Figure 1 illustrates the portion of the whole system that was modelled in SINDA/FLUINT. There were two wall temperature measurements (upstream and downstream) in the test section, as well as two pressure measurements. Figure 2 shows the representation of this section as modelled in SINDA/FLUINT.

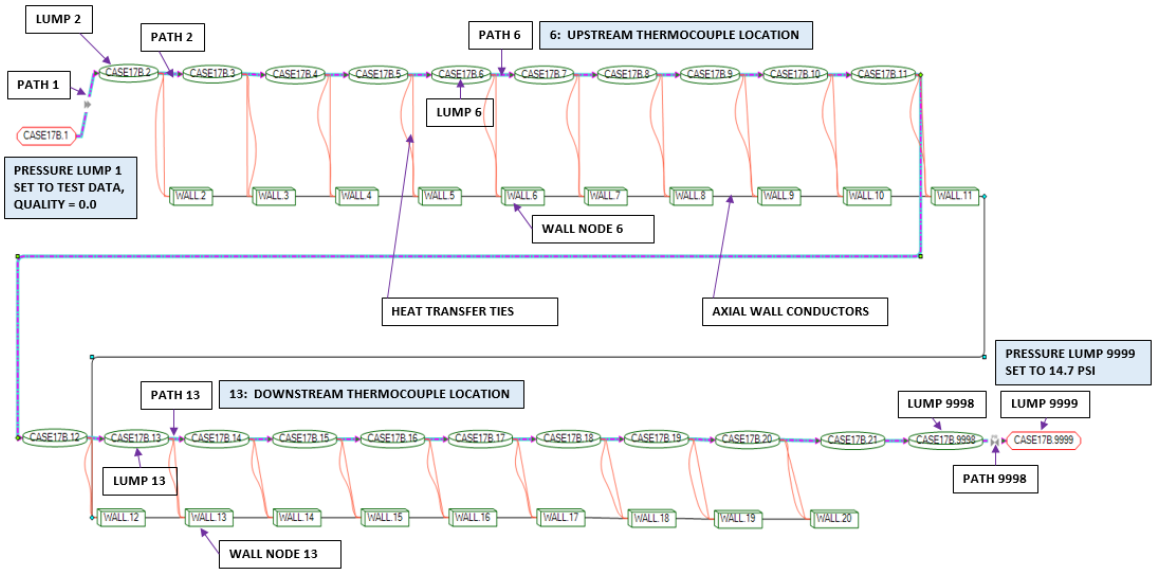

Figure 2: SINDA/FLUINT Flow Schematic of the Liquid Nitrogen Test Section Showing SINDA/FLUINT Fluid LUMPS, Flow PATHS, Wall NODES, Heat Transfer TIES, and Pipe Axial CONDUCTORS

LUMP 6 and LUMP 13 represent approximately the location of the upstream and downstream wall temperatures respectively in the test section. The model inlet, location A in Figure 1, used test pressure measurements at the location, as well as a quality of 0.0. This inlet condition was imposed on LUMP 1 (a SF PLENUM). The model outlet LUMP 9999 (a SF PLENUM), location B in Figure 1, assumed an exit pressure of 14.7 psi. Since this pressure was not the correct pressure at this point in the system, a pressure regulator was placed between LUMP 9998 and LUMP 9999. This was to account for all the losses in the line that were not modelled, downstream of the test section to the exhaust vent to atmosphere. The piping system parameters are shown in Table 1. SINDA/FLUINT TIES were used to model the heat transfer, thereby using the default heat transfer correlations in SINDA/FLUINT. The University of Florida's correlations were implemented using SINDA/FLUINT HTU TIES (user defined heat transfer).

PIPE LENGTH	**22.5 IN (57.2 CM)**
PIPE OD	**0.5 IN (1.27 CM)**
PIPE ID	**0.46 IN (1.168 CM)**
WALL THICKNESS	**0.02 IN (0.0508 CM)**
WALL MASS	**0.184 LBM (0.0836 KG)**
MATERIAL	**SS 304**

Table 1: SINDA/FLUINT Piping Parameters of Liquid Nitrogen Test Section

In the liquid nitrogen test cases the flow rate was measured far downstream of the test section, near the system exit. Thus the flow rate measurements did not accurately reflect the flow rate in the test section during the start of the chill-down at the entrance of the test section. SINDA/FLUINT was highly sensitive, and sometime unstable, setting the test flow rate downstream (the outlet) of the test section model and setting the test pressure upstream (the inlet) of the test section model. This sensitivity lead to higher flow rate oscillations at the entrance of the model's test section. In all cases, where either the upstream or downstream flow rate was set, the inlet pressure was taken from test data. In the downstream flow rate set case this was an upstream boundary condition. In the upstream flow rate set case, which was more stable than the downstream flow rate set case, this pressure was used as an inlet (SINDA/FLUINT plenum) to set the thermodynamic state (temperature and quality) coming into the system. Again noting that using the set upstream flow rate boundary condition, with a flow rate that was measured downstream, was not representative of the actual flow that would be occurring at the inlet of the test section.

The University of Florida's heat transfer empiricisms, as implemented in SINDA/FLUINT for the liquid nitrogen test cases, were sensitive to these mass flow rate oscillations. In some cases this sensitivity caused significant deviations from test data. However internal heat transfer calculations used by SINDA/FLUINT did not reflect the same sensitivity. The cause of the University of Florida's heat transfer calculation's sensitivity was due to the film boiling regime being proportional to the flow rate raised to the fourth power. This correlation calculated high values for heat transfer in the film boiling regime that caused chill-down of the wall to occur too rapidly at the start of the chill-down. The heat transfer empiricisms calculated by the University of Florida were based on flow rates that were measured far downstream of the test section. If potential oscillations in the flow (over the nominal flow rate measured at the system's exit) were actually occurring in the test section (especially the inlet) and not just an artifact of the numerical solution, then the empiricisms would over predict the wall heat transfer at these locations.

Unfortunately, when the SINDA/FLUINT model set the flow rate upstream of the test section, the pressure downstream at the test section's exit needed to be known. Pressures were measured in the tests at a downstream location of the test section. When the pressure measured at the downstream location of the test section was used as the model's exit pressure, unrealistically high flow rates were obtained. Thus the associated chill-down rates were excessively high. The pressure drops predicted by SINDA/FLUINT for the downstream set flow rate boundary condition were much smaller than test section measured pressure drops. It was speculated that multiphase pressure drop correlations used internally in SINDA/FLUINT may need to be adjusted. However in order to get the magnitude of the flow rate measured in the system (albeit a far downstream flow rate) for the model which used an upstream flow rate boundary condition, an exit pressure needed to be assumed that did not match the test data pressure. Models that were run with an upstream flow rate set as a boundary condition therefore assumed a pressure drop that was small.

The magnitude of this pressure drop was obtained by running the models with a downstream flow rate boundary condition with the inlet pressure set to be that of the test.

The SINDA/FLUINT PATHS used in the model were primarily STUBE CONNECTORS. However, sometimes the model depending on the case, required TUBES for stability. The maximum time step, DTMAXF, was set to 1e-4 sec. The SINDA/FLUINT LUMPS used were TANKS.

IV. Liquid Hydrogen Chill-Down

A schematic of the liquid hydrogen chill-down system is shown in Figure 3. Only a portion of the system was modelled as illustrated. A set flow rate boundary at the inlet location SD16 (Figure 3) was used. This flow rate was obtained from test data. Since there was no pressure measurement at SD16, the inlet pressure was assumed to be the value taken at location PT3 (Figure 3) where the pressure was measured. The outlet condition used the test pressure data from location PT4 (Figure 3). Since a set inlet flow rate was specified as the boundary condition, the pressure at the inlet, set to PT3 as well as the quality being set equal to zero, were used to determine the thermodynamic state coming into the system. However because of all the valves and manifold piping occurring upstream of location SD16, a quality of zero may not realistically be the case. The SINDA/FLUINT model schematic of the high-lighted section, shown in Figure 3, is illustrated in Figure 4. Piping system parameters are shown in Table 2.

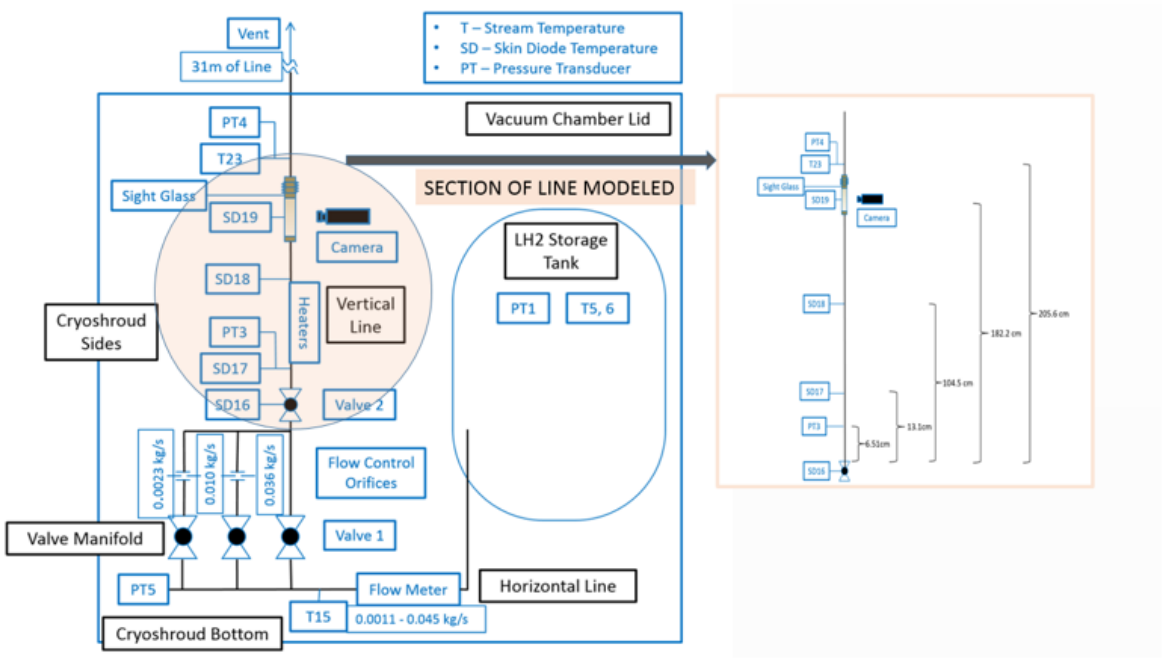

Figure 3: Liquid Hydrogen Chill-down System

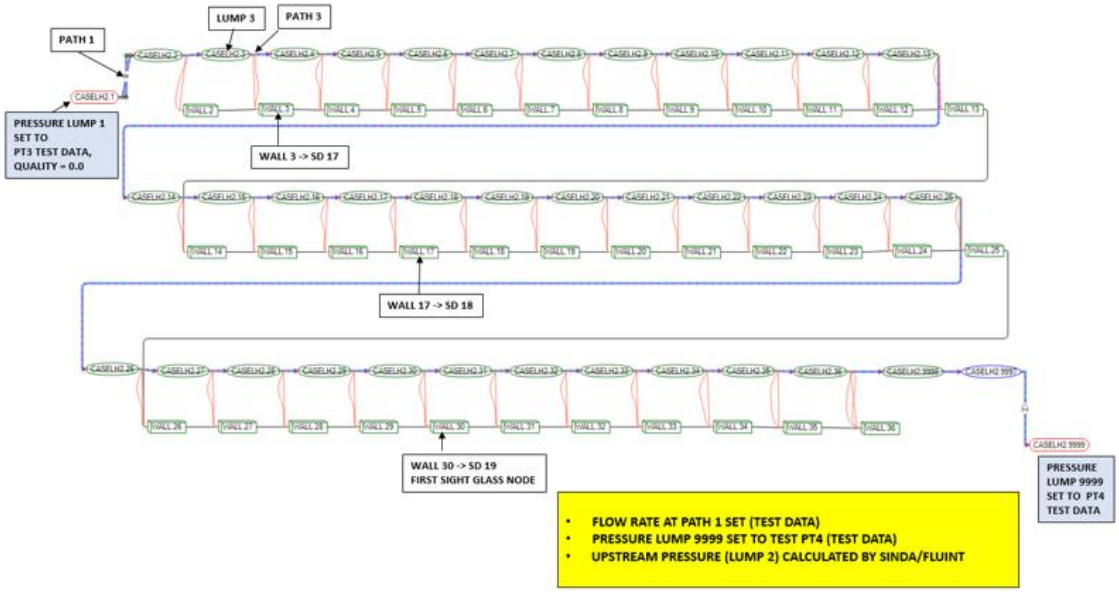

Figure 4: SINDA/FLUINT Flow Schematic of the Liquid Hydrogen Test Section Showing SINDA/FLUINT Fluid LUMPS, Flow PATHS, Wall NODES, Heat Transfer TIES, and Pipe Axial CONDUCTORS

Line OD	0.012700025	[m]
Line ID	0.01021	[m]
Length from inlet to skin temperature SD17	0.37148	[m]
Length from inlet to skin temperature SD18	1.285875	[m]
Length from inlet to skin temperature SD19	2.06375	[m]
Length from inlet to stream temperature SD23	2.29	[m]
Length from inlet to P3	0.30798	[m]
Length from inlet to P4	2.29	[m]
Length (approximate) from SD23/P4 to Vent	31	[m]
Total length of straight, vertical section of transfer line	2.29	[m]
Length of SG can/housing	0.15	[m]
Resultant Length of SS pipe	2.14	[m]
Density of 304 SS	8030	[kg/m^3]
Mass of flow control manifold (4 orifices, 6 valves, 6 blocks)	11.4	[kg]
Total mass of Sight glass can/housing	1.931818182	[kg]
Effective mass of Sight glass can/housing	0.579545455	[kg]
Mass of SS tubing	0.769925224	[kg]
Total mass of transfer line	4.110743406	[kg]
Total effective mass of vertical transfer line	2.758470678	[kg]

Table 2: SINDA/FLUINT Piping Parameters of Liquid Hydrogen Test Section (Vertical Portion of Line)

In the liquid hydrogen test cases the flow rate was measured upstream, so all cases were run with an upstream set mass flow rate. The inlet pressure of the system was taken from a test pressure measurement taken at the inlet of the test section. As with the liquid nitrogen test cases, using system pressures to drive the flow rate solution caused wall chill-down to occur at a faster rate because the flow rate calculated by SINDA/FLUINT was significantly larger than the test data flow rate.

Both the University of Florida's heat transfer correlations and SINDA/FLUINT's internal correlations faired similarly to wall temperature test data. They were acceptable although improvements could be made to the University of Florida correlations as well and SINDA/FLUINT's internal correlations.

The SINDA/FLUINT PATHS used in the model were primarily STUBE CONNECTORS. However a SINDA/FLUINT TUBE was used as the second PATH in the system (after the set inlet flow rate shown as PATH 1

in Figure 4) for stability. The maximum time step, DTMAXF, was set to 1e-4 sec, although some cases that had excessive flow reversal DTMAXF was set to 1e-5 sec. The SINDA/FLUINT LUMPS used were TANKS.

V. Heat Transfer Correlations

The University of Florida's correlation for the film boiling heat transfer regime is[3]:

$$Nu = c_1\left[1+\left(\frac{1}{\frac{L}{D}+0.1}\right)^{c_2}\right]\left(\frac{GD}{\mu_v}\right)^{c_3}\mathrm{Pr}_v^{c_4}\,erf\left(\frac{X_E+1}{\log_{c_5}\mathrm{Re}_v}\right)^{c_6}\left(\frac{\mu_v}{\mu_{v,wall}}\right)^{c_7} + c_8\left(\frac{k_1}{k_v}\right)\exp\left(-\left(\frac{L}{D}\right)^{c_9}\right)We_D^2\left[\frac{h_{fg}}{c_{p,v}(T_w-T_{sat})}\right] \tag{1}$$

The University of Florida's correlation for the transition boiling heat transfer regime is[3]:

$$h_{tp} = c_0\,\mathrm{Pr}_l^{c_1}\,Xh_{nb} \tag{2a}$$

$$X = 10.37\text{-}36.93\theta + 47.49\theta^2\text{-}20.82\theta^3 \tag{2b}$$

$$\theta = \frac{T_w - T_{sat}}{T_{wet} - T_{sat}} \tag{2c}$$

The University of Florida's correlation for the nucleate boiling heat transfer regime is (include Dittus-Boelter for single phase liquid) [3]:

$$h_{nb} = c_1\,\mathrm{Pr}_l^{c_2}\,Ja^{c_3}We_D^{c_4}\left[\frac{\rho_l g(\rho_l-\rho_v)D^3}{\mu_l^2}\right]^{c_5} h_{sp,l} \tag{3}$$

$$h_{sp,l} = 0.023\frac{k_l}{D}\mathrm{Re}_l^{0.8}\,\mathrm{Pr}_l^{0.4} \tag{4}$$

The critical heat flux is defined by [3]:

$$q''_{CHF} = c_1 G h_{fg} We_L^{-0.5}\left(\frac{\rho_l}{\rho_v}\right)^{-0.91}\left(\frac{L}{D}\right)^{0.48}\left(1+0.07We_L^{0.35}\frac{\Delta h_{sub}}{h_{fg}}\right) \tag{5}$$

where the enthalpy subcooling is relative to the inlet.

The rewet temperature is defined by[3]:

$$T_{wet} = \frac{27}{32}T_{cr}\left(1+c_1We_D^{c_2}Re_l^{c_3Ja^{c_4}}\right) \tag{6}$$

The process for determining the heat transfer regime is outlined in Figure 5.

Calculate *Twet* prediction for the given mass flow rate and local pressure

A If $Tw > Twet$ then $h = hfb$

B If $Tw < Twet$, then:

1. If $Tw >$ Tsat, then:
   a) Calculate $q"CHF$ prediction
   b) Calculate $q"nb$ prediction
      i) If $q"nb > q"CHF$ then $h = htb$
      ii) If $q"nb < q"CHF$ then $h = hnb$
2. If $Tw < Tsat$ then $h = hDB$

Figure 5: University of Florida Criteria for Heat Transfer Regime

A summary flow chart of SINDA/FLUINT's methodology for calculating heat transfer coefficients using SINDA/FLUINT TIES is outlined in Figure 6. A detailed description of equations and methodology can be found in the SINDA/FLUINT User's Manual[4]. SINDA/FLUINT uses the Chen correlation for nucleate boiling, and for film boiling, a correlation by Bromley for low quality flows and a correlation by Groeneveld for high quality flows.

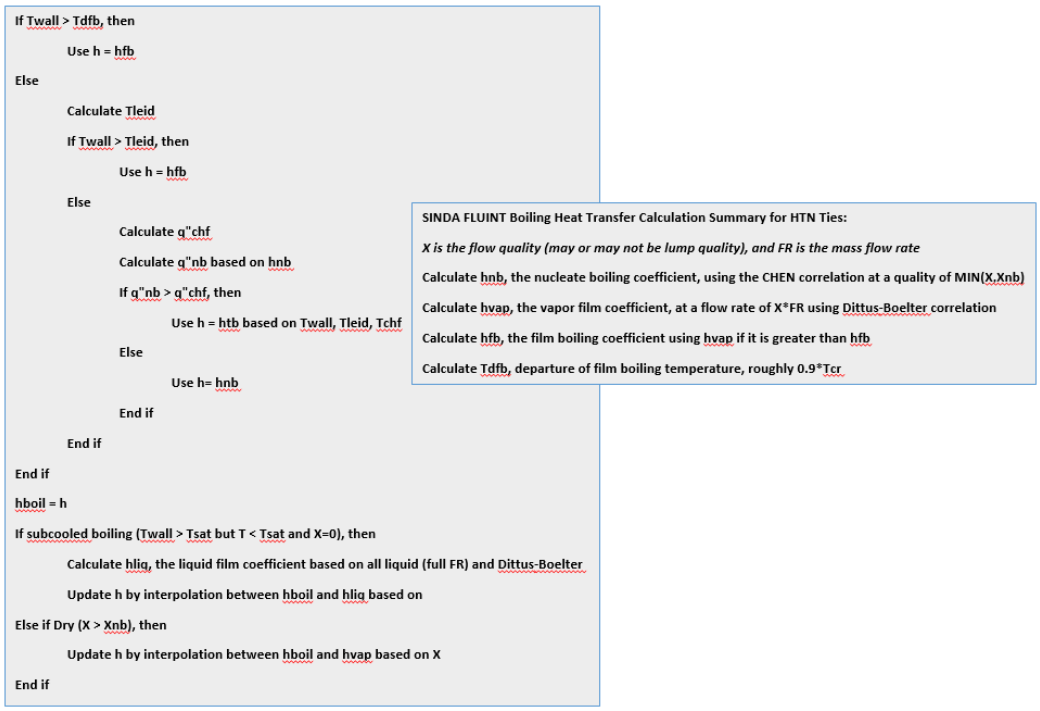

Figure 6: SINDA/FLUINT Criteria for Heat Transfer Regime

A modification by Shah[5] was added to the standard heat transfer correlations used by SINDA/FLUINT. This modification is used during film boiling on the default Dittus-Boelter correlation for gas convective heat transfer. It was employed in the liquid hydrogen chill-down test cases. The Shah modification is a multiplication factor on the Dittus-Boelter equation:

$$S = 0.046\ F\ (T_v/T_w)^{0.55} \qquad (7a)$$

$$F = 8.53\ (L/D)^{-0.63} \qquad L/D <= 30.0 \qquad (7b)$$

$$F = 1.0 \qquad L/D >= 30.0 \qquad (7c)$$

VI. Results

A. Liquid Nitrogen Chill-Down: Horizontal Flow

Table 3 illustrates the liquid nitrogen chill-down cases' Reynolds numbers for horizontal flow.

LN2 HORIZONTAL	REYNOLDS NUMBER
CASE 17b	23677
CASE 26b	132597
CASE 21b	3743

Table 3: Reynolds Number for Nitrogen Chill-down Horizontal Flow Cases

Figures 7 through 9 show the wall temperature results for the horizontal flow liquid nitrogen chill-down cases. Except for the lower Reynolds number case, Case 21b, the cases using the UF heat transfer correlations showed a greater sensitivity to what flow rate boundary condition was used (i.e. upstream or downstream). The SF internal correlations did not show much sensitivity between the flow rate boundary conditions. The largest deviation from test data occurred with Case 26b (highest Reynolds number) for the case of a downstream flow rate set condition. The interesting to note in Case 26b, were the flow rates at the upstream end of the test section (SF PATH 6) for this downstream flow rate set condition (Figure 10). The model using the SF TIES (internal heat transfer correlations) had flow rate results that were larger and more oscillatory than the flow rate results using the UF heat transfer correlations, yet the heat transfer from the wall was significantly greater for the UF results. Figure 8a shows the wall temperature at the upstream test location for the UF model results dropping significantly faster than the test data or the SF model results. Equation 1 shows that the film boiling heat transfer coefficient is proportional to the Weber number squared which translates to being proportional to the flow rate raised to the fourth power. The inlet to the chill-down test section could possibly be subject to large flow oscillations and this UF correlation shows possible sensitivity to these large fluctuations. Figure 11 overlays the wall temperature with the heat transfer coefficients (PATH 6, NODE 6). There are a couple of isolated heat transfer spikes in the model using the SF TIES, but these spikes are not being translated to rapid wall chill-down. In fact the chill-down temperature slope is remarkably reduced compared to the test data's temperature slope. There are sustained larger calculated values of the heat transfer coefficient using the UF film boiling correlation, causing the wall temperature to chill-down rapidly.

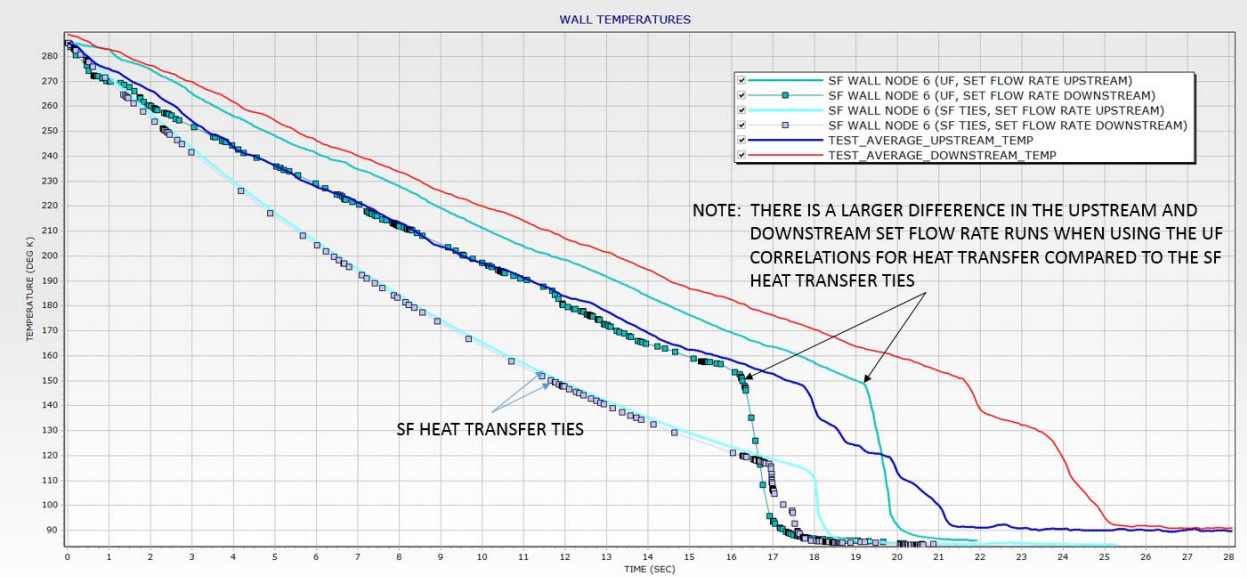

Figure 7a: Horizontal Liquid Nitrogen Chill-down (17B) UF and SF Heat Transfer Wall Temperature Results at Upstream Test Location

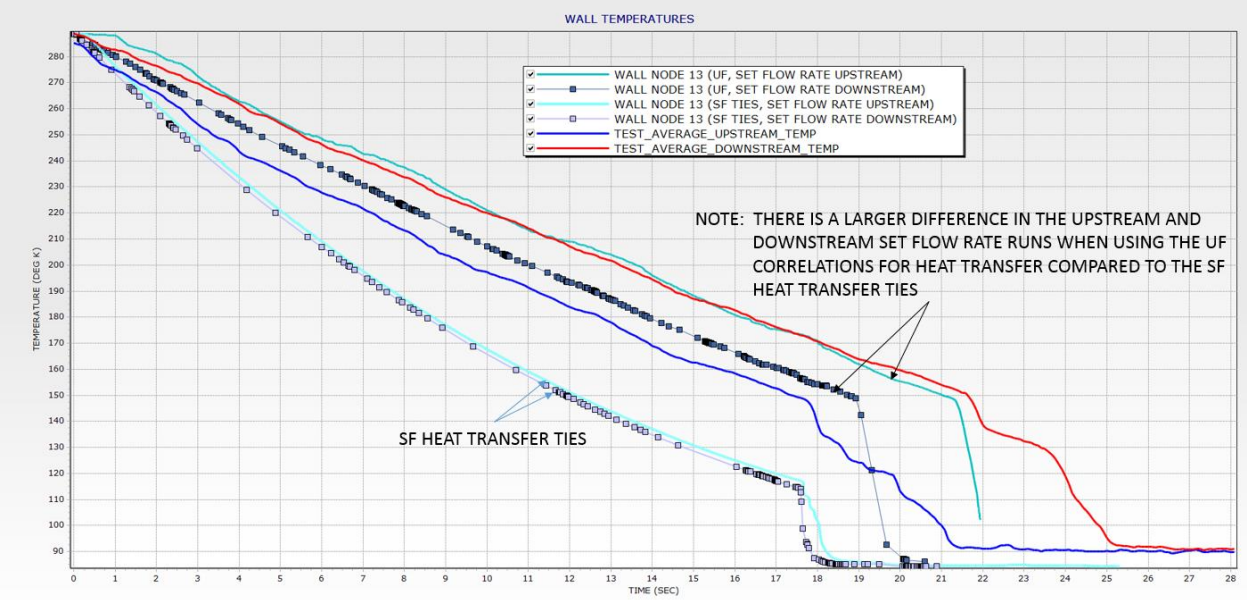

Figure 8b: Horizontal Liquid Nitrogen Chill-down (17B) UF and SF Heat Transfer Wall Temperature Results at Downstream Test Location

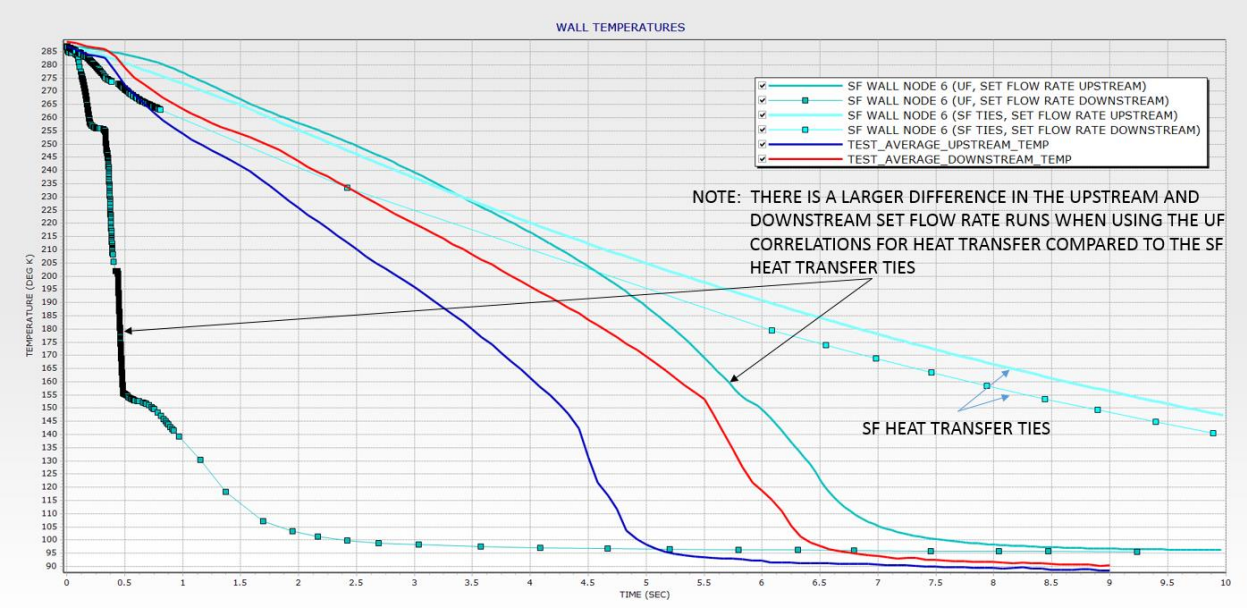

Figure 8a: Horizontal Liquid Nitrogen Chill-down (26b) UF and SF Heat Transfer Wall Temperature Results at Upstream Test Location

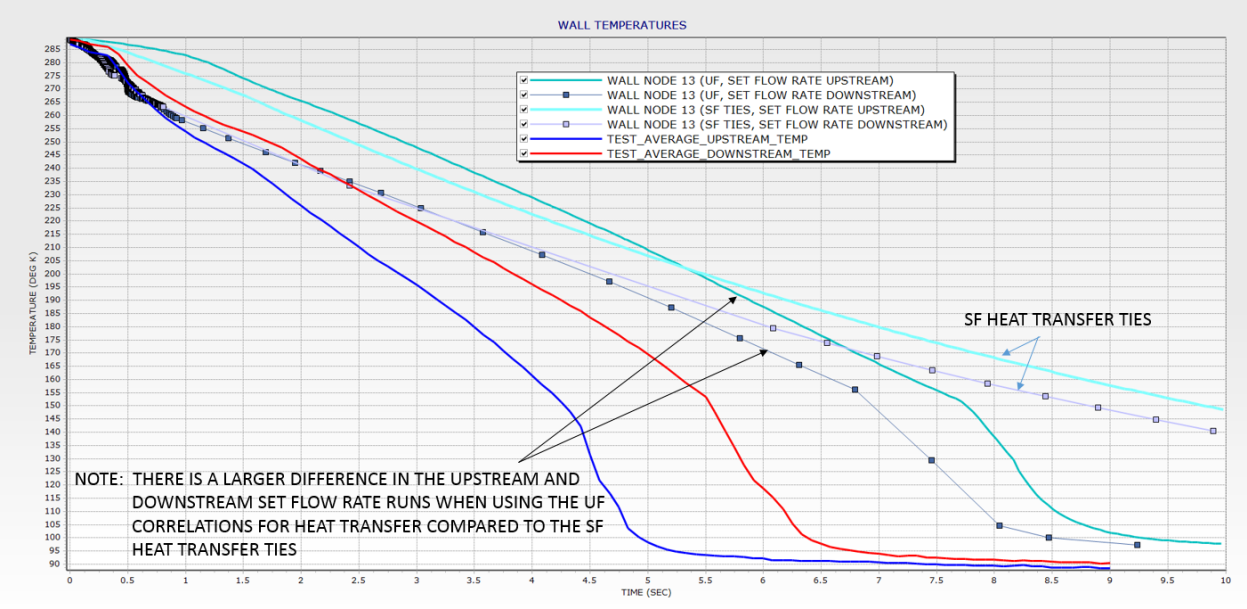

Figure 8b: Horizontal Liquid Nitrogen Chill-down (26b) UF and SF Heat Transfer Wall Temperature Results at Downstream Test Location

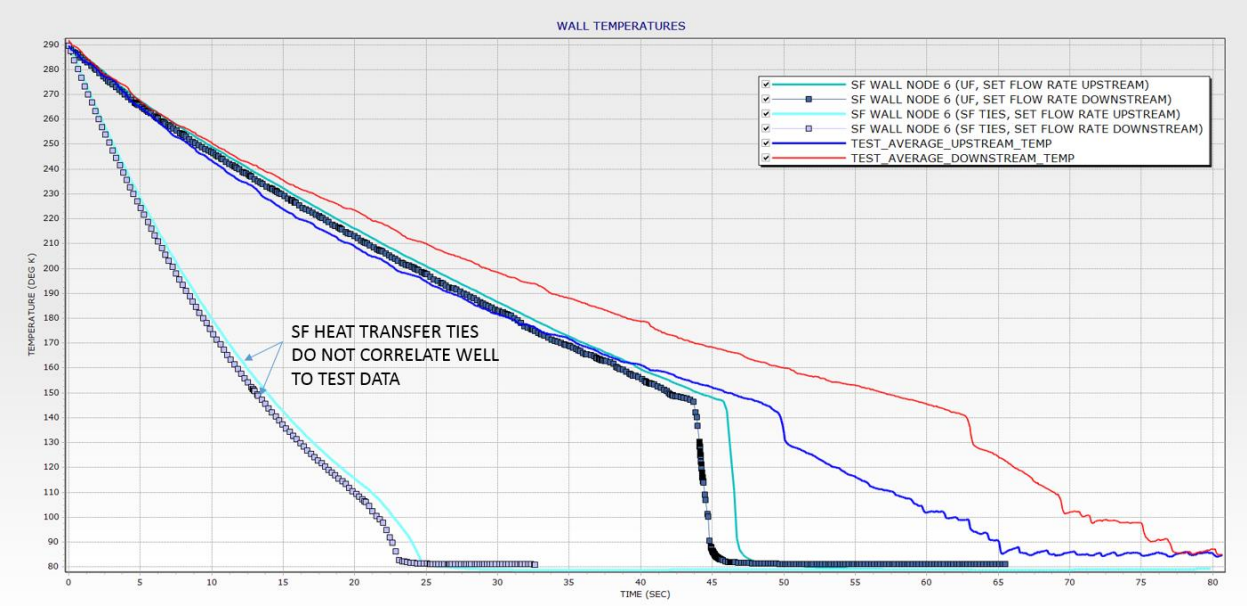

Figure 9a: Horizontal Liquid Nitrogen Chill-down (21b) UF and SF Heat Transfer Wall Temperature Results at Upstream Test Location

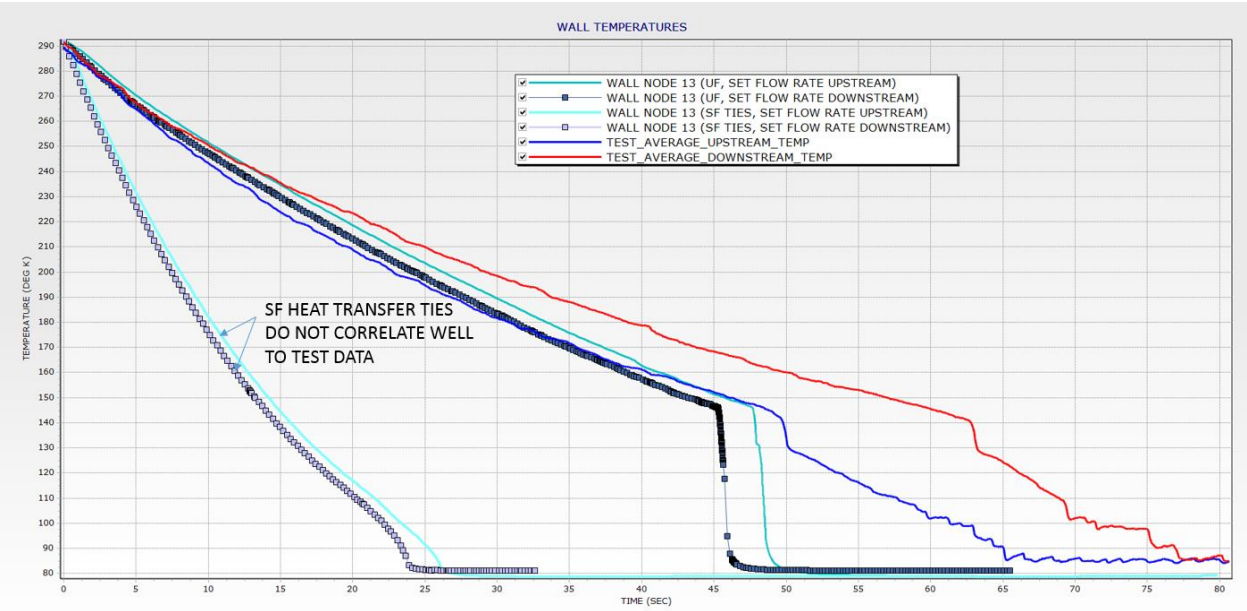

Figure 9b: Horizontal Liquid Nitrogen Chill-down (21b) UF and SF Heat Transfer Wall Temperature Results at Downstream Test Location

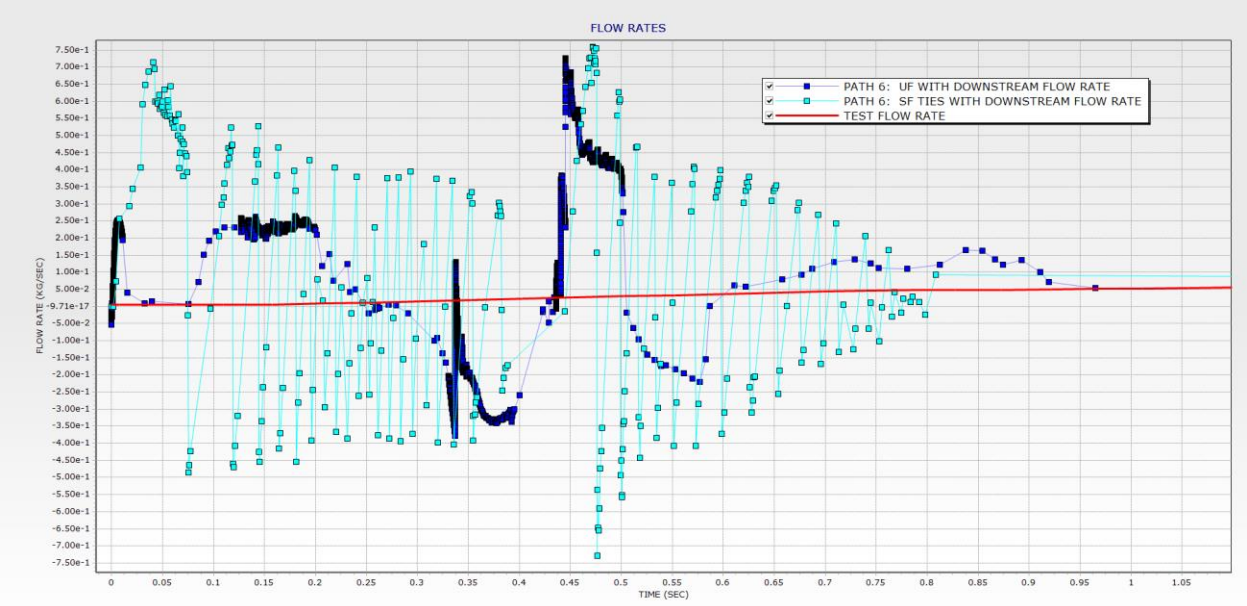

Figure 10: Horizontal Liquid Nitrogen Chill-down (26b) UF and SF Heat Transfer Flow Rate Results at the Upstream Test Location for Set Flow Rate Downstream Boundary

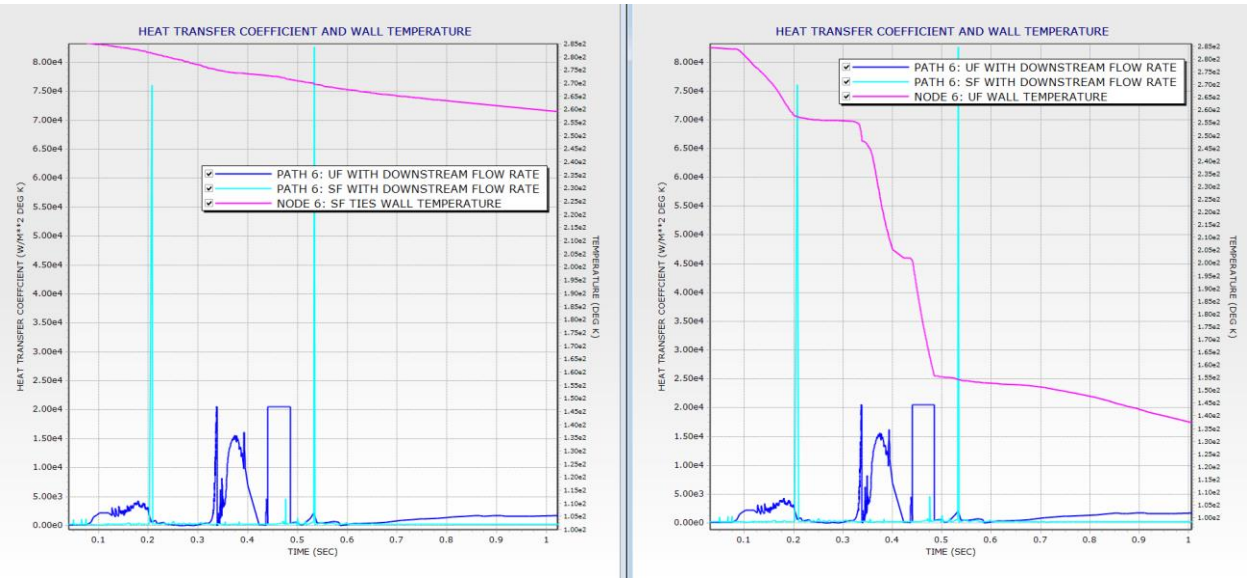

Figure 11: Horizontal Liquid Nitrogen Chill-down (26b) UF and SF Heat Transfer Flow Rate and Heat Transfer Coefficient Results at the Upstream Test Location for Set Flow Rate Downstream Boundary

Figures 12 through 14 show the phase change heat transfer regimes for Cases 17b, 26b, and 21b. As expected for case 26b using the SF TIES (both downstream and upstream flow rate boundaries), the heat transfer regime stays in film boiling. Case 26b using the UF correlations (with downstream flow rate) shows immediate transition boiling and nucleate boiling onset. This did not occur when the upstream flow rate boundary condition was utilized.

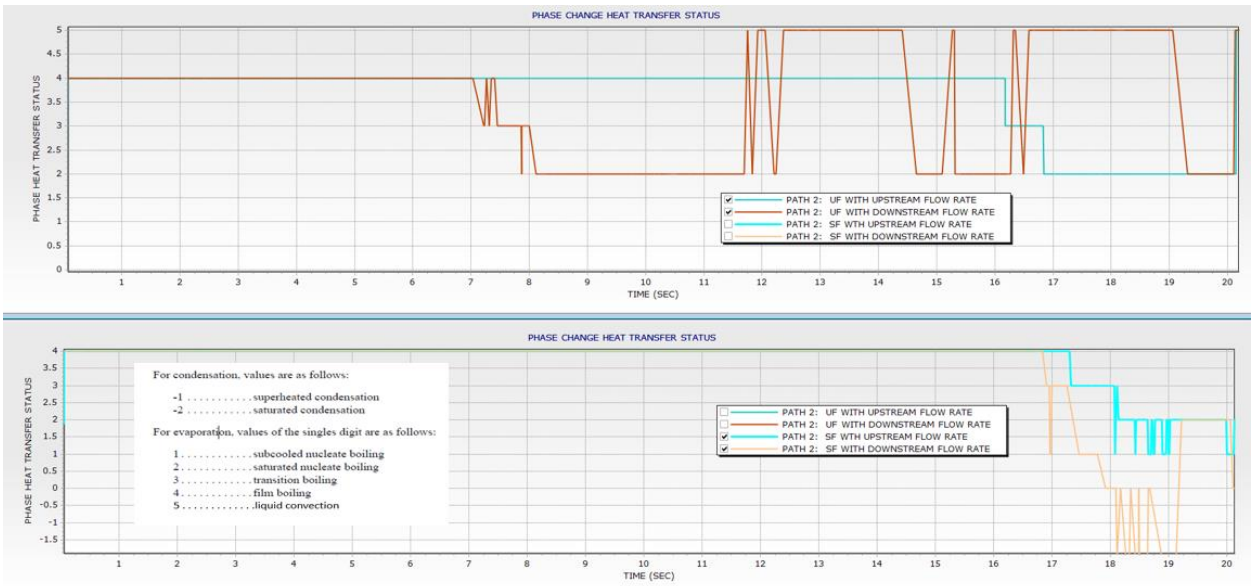

Figure 12: Horizontal Liquid Nitrogen Chill-down (17b) UF and SF Heat Transfer Regime at Test Section Inlet

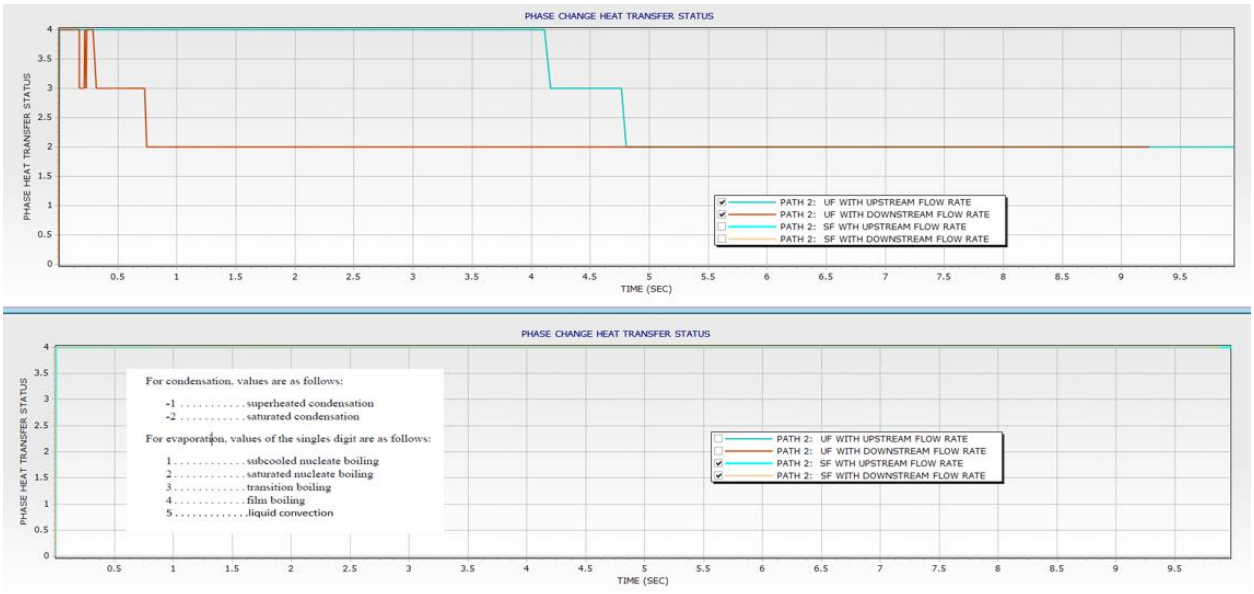

Figure 13: Horizontal Liquid Nitrogen Chill-down (26B) UF and SF Heat Transfer Regime at Test Section Inlet

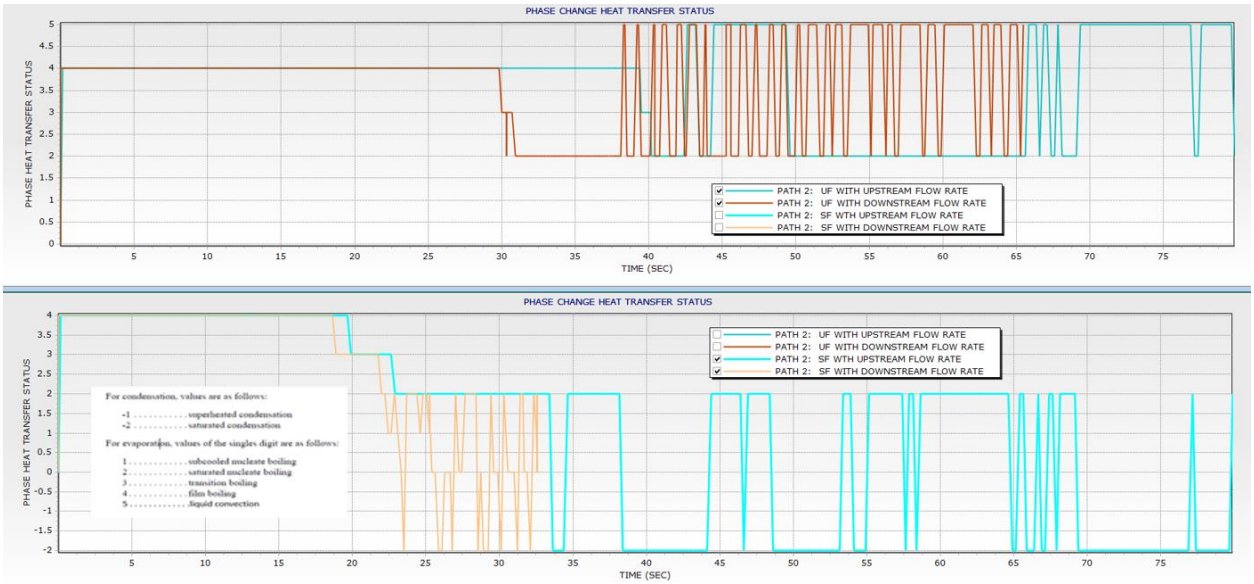

Figure 14: Horizontal Liquid Nitrogen Chill-down (21b) UF and SF Heat Transfer Regime at Test Section Inlet

It should be noted that the test section pressures did not correspond to numerical results whether SF TIES were used or the UF correlations. Figure 15 shows pressure results for CASE 17b using UF correlations (both upstream and downstream flow rate boundaries). Please refer to Figure 2 for LUMP identifications. Figure 15 shows very small pressure drops through the system. The test data pressure drop, PT1 to PT2, could not be obtained. Attempts to force this pressure drop caused the model to become unstable. Similar behavior was observed for CASE 17b using SF TIES, Figure 16, as well as all other liquid nitrogen test cases.

Figure 15: Horizontal Liquid Nitrogen Chill-down (17b) UF Heat Transfer with Pressures through the Test Section (Upstream and Downstream Flow Rate Boundaries)

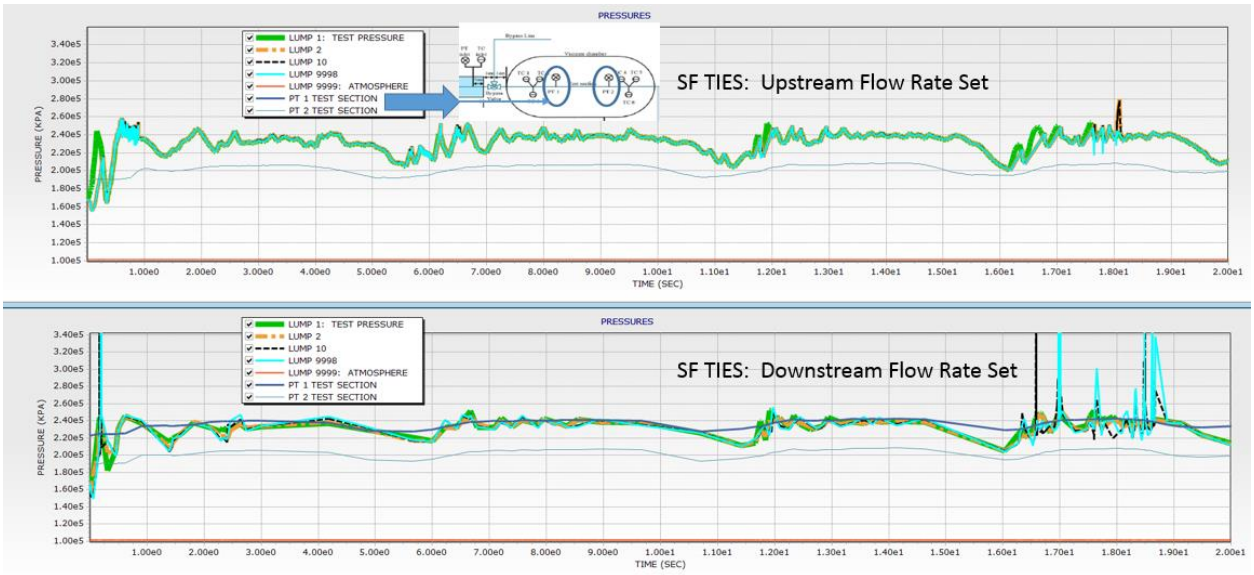

Figure 16: Horizontal Liquid Nitrogen Chill-down (17b) SF TIES Heat Transfer with Pressures through the Test Section (Upstream and Downstream Flow Rate Boundaries)

B. Liquid Nitrogen Chill-Down: Vertical Downward Flow

The model set up is that of Figure 2 but hydrostatic heights were incorporated onto the SF LUMPS. Table 4 shows the cases that were modelled as well as their corresponding Reynolds numbers. Figures 17 through 20 include both upstream and downstream wall temperature plots. Figures 21 through 22 show only the upstream wall temperature plots.

LN2 VERTICAL DOWNWARD	REYNOLDS NUMBER
CASE 29	13350
CASE 12	93740
CASE 25	126423
CASE 2	45227
CASE 39*	4164
CASE 50*	17362

Table 4: Reynolds Number for Nitrogen Chill-down Vertical Downward Flow Cases
***Only Upstream Wall Temperature Plots are Included**

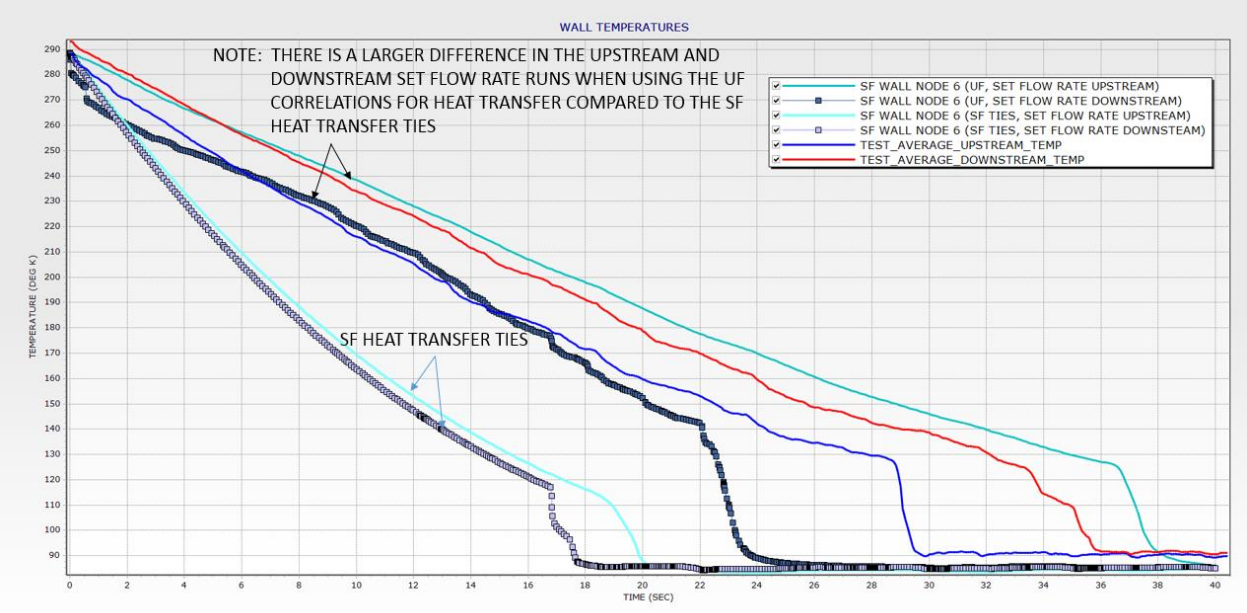

Figure 17a: Vertical Downward Liquid Nitrogen Chill-down (29) UF and SF Heat Transfer Wall Temperature Results at Upstream Test Location

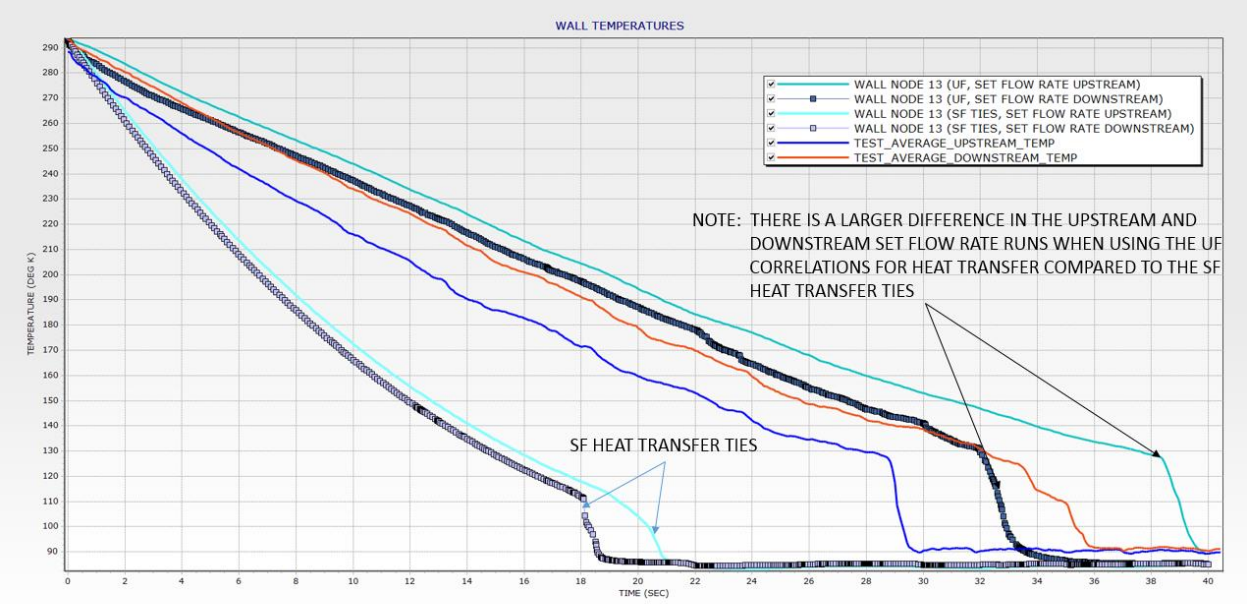

Figure 17b: Vertical Downward Liquid Nitrogen Chill-down (29) UF and SF Heat Transfer Wall Temperature Results at Downstream Test Location

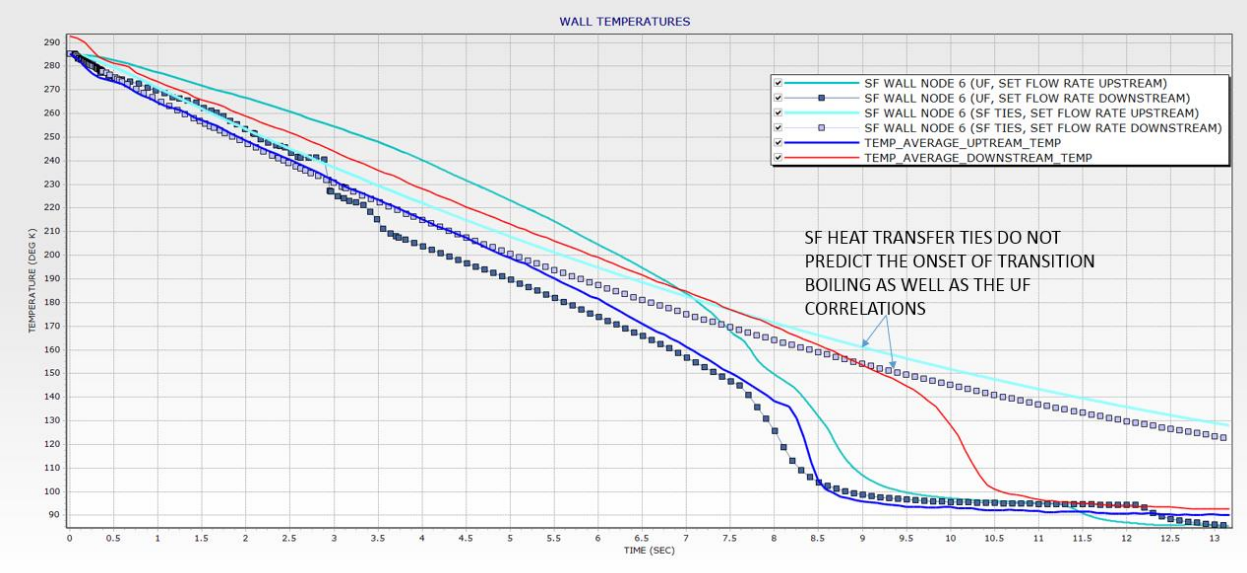

Figure 18a: Vertical Downward Liquid Nitrogen Chill-down (12) UF and SF Heat Transfer Wall Temperature Results at Upstream Test Location

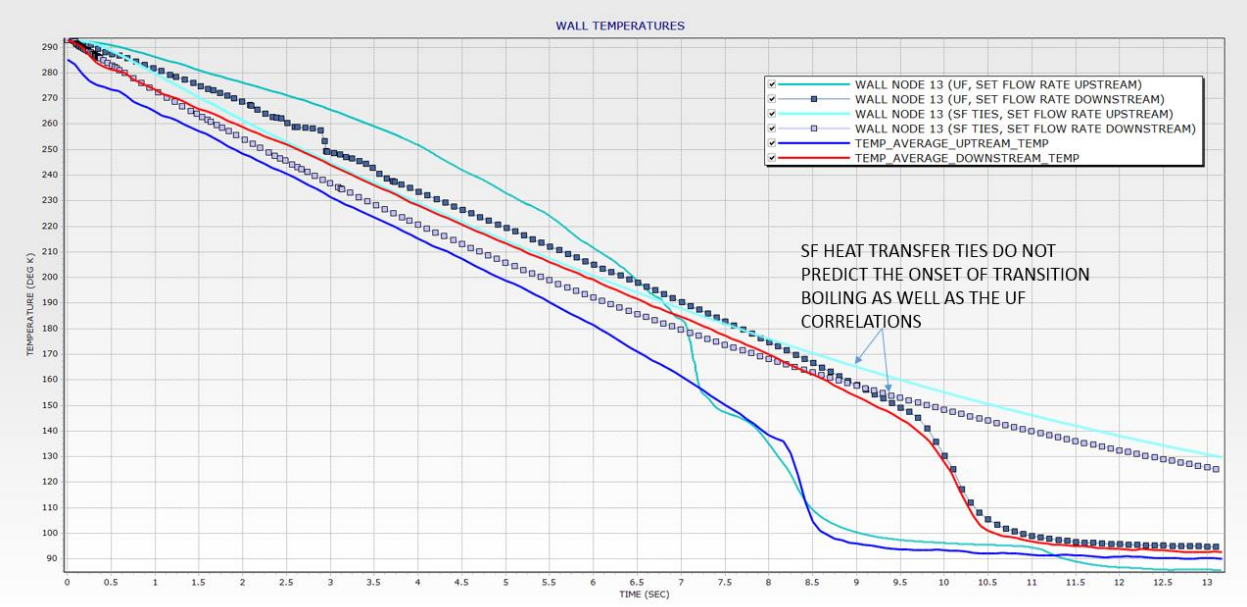

Figure 18b: Vertical Downward Liquid Nitrogen Chill-down (12) UF and SF Heat Transfer Wall Temperature Results at Downstream Test Location

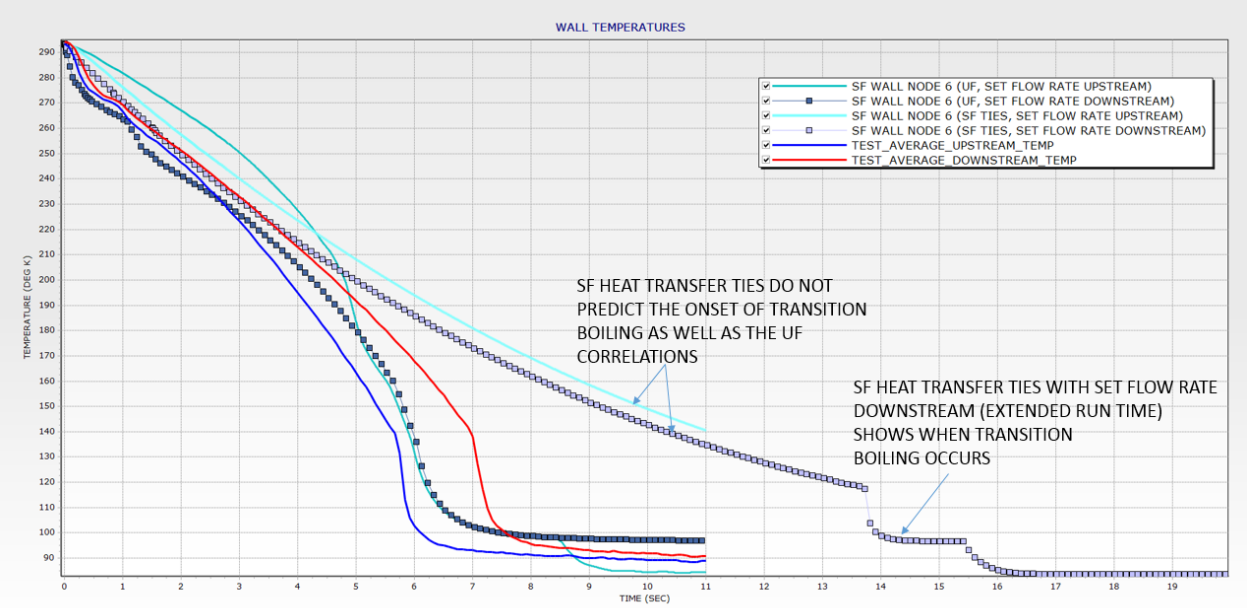

Figure 19a: Vertical Downward Liquid Nitrogen Chill-down (25) UF and SF Heat Transfer Wall Temperature Results at Upstream Test Location

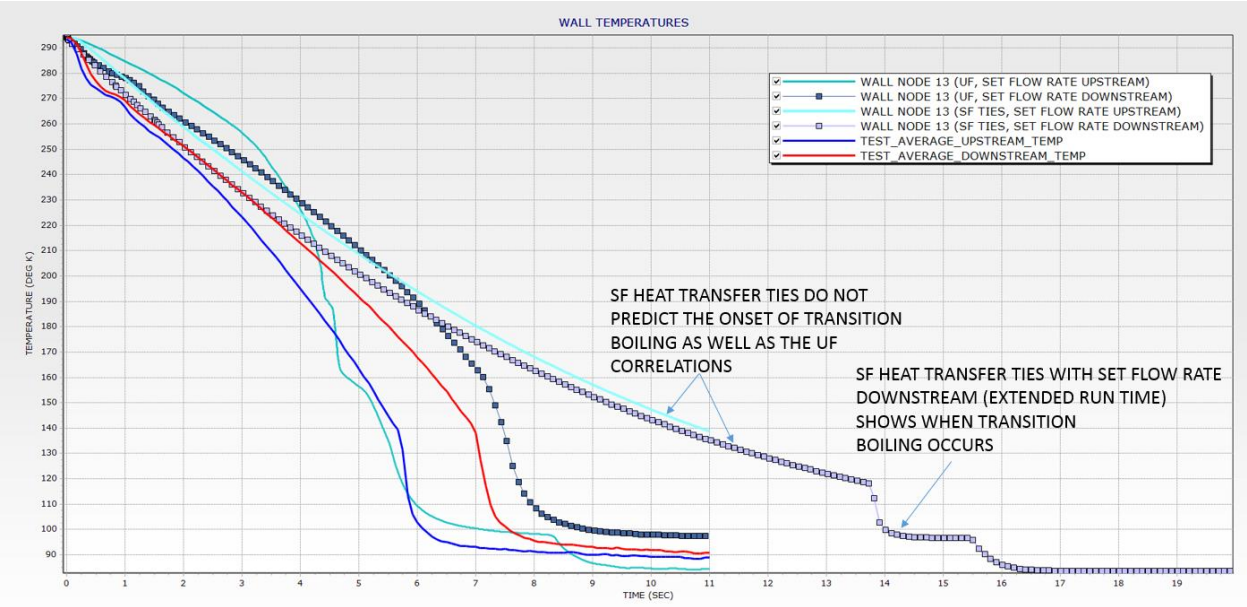

Figure 19b: Vertical Downward Liquid Nitrogen Chill-down (25) UF and SF Heat Transfer Wall Temperature Results at Downstream Test Location

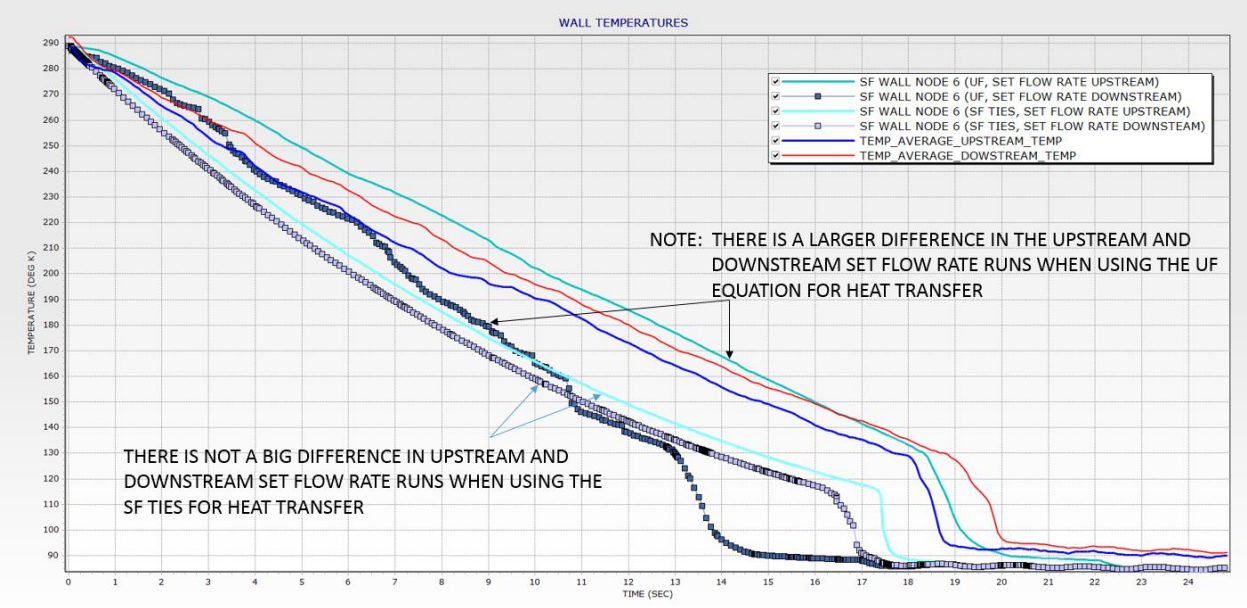

Figure 20a: Vertical Downward Liquid Nitrogen Chill-down (2) UF and SF Heat Transfer Wall Temperature Results at Upstream Test Location

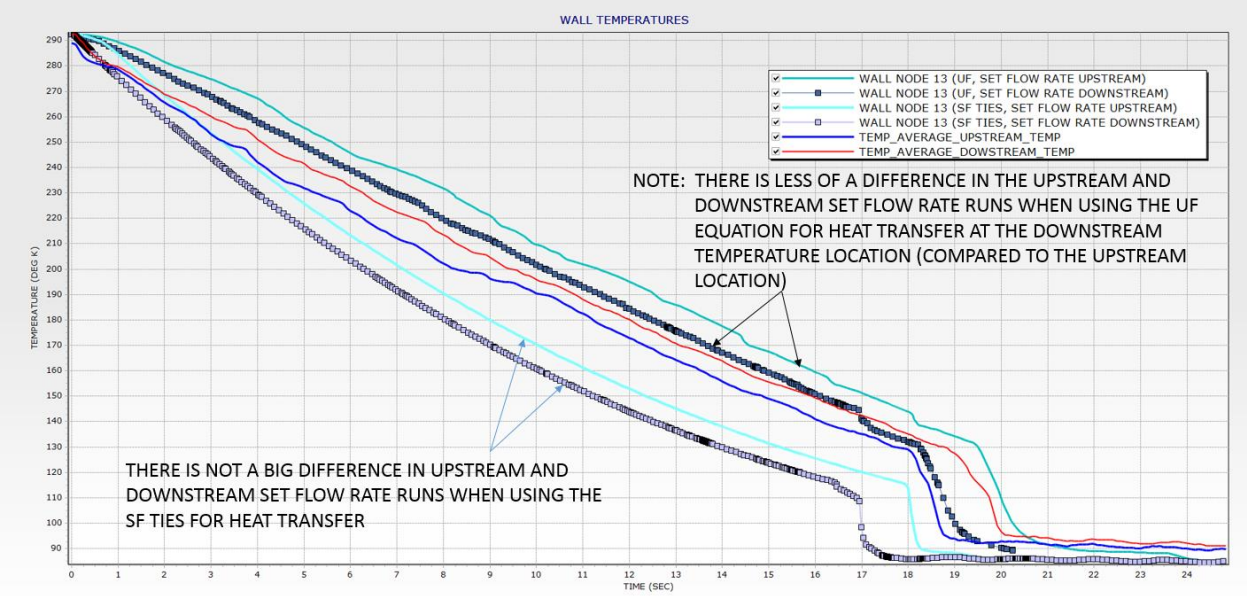

Figure 20b: Vertical Downward Liquid Nitrogen Chill-down (2) UF and SF Heat Transfer Wall Temperature Results at Downstream Test Location

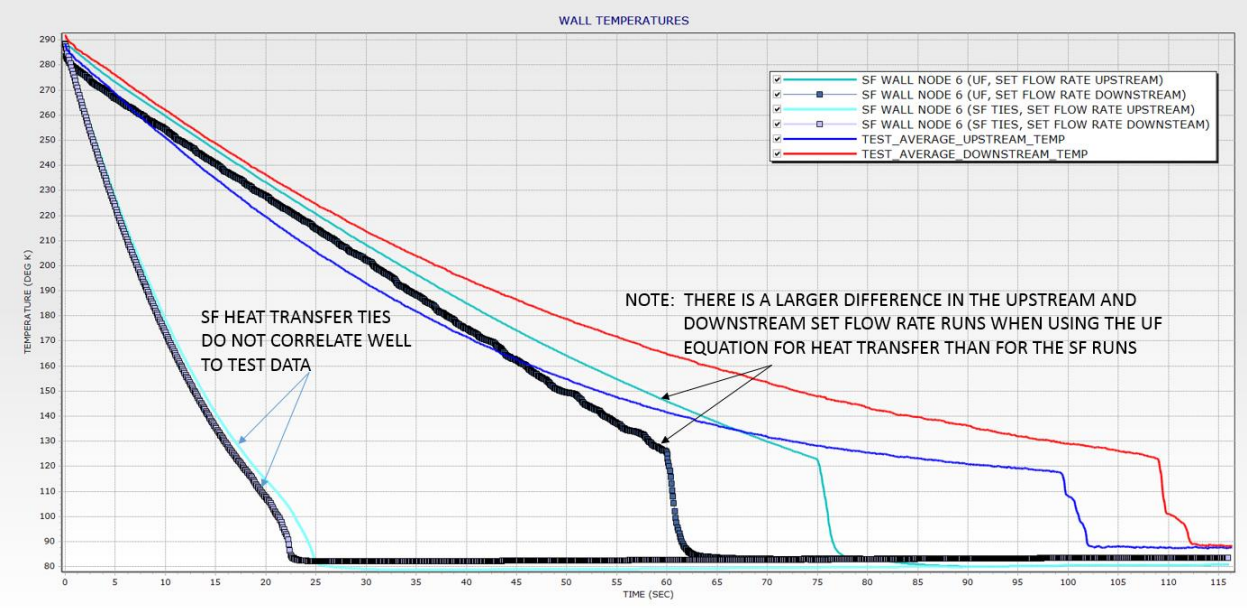

Figure 21: Vertical Downward Liquid Nitrogen Chill-down (39) UF and SF Heat Transfer Wall Temperature Results at Upstream Test Location

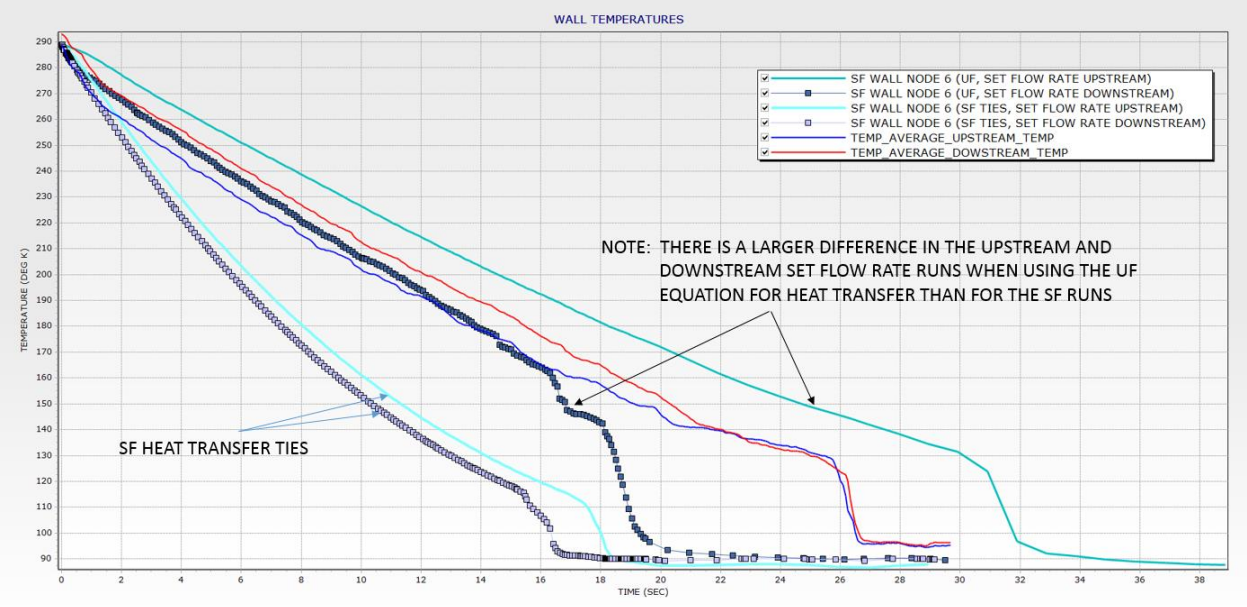

Figure 22: Vertical Downward Liquid Nitrogen Chill-down (50) UF and SF Heat Transfer Wall Temperature Results at Upstream Test Location

C. Liquid Nitrogen Chill-Down: Vertical Upward Flow

The model set up is that of Figure 2 but hydrostatic heights were incorporated onto the SF LUMPS. Table 5 shows the cases that were modelled as well as their corresponding Reynolds numbers. Figures 23 through 28 show only the upstream wall temperature plots.

LN2 VERTICAL UPWARD	REYNOLDS NUMBER
CASE 29*	98037
CASE 12*	14785
CASE 25*	19731
CASE 2*	24202
CASE 39*	113303
CASE 50*	3454

Table 5: Reynolds Number for Nitrogen Chill-down Vertical Upward Flow Cases
***Only Upstream Wall Temperature Plots are Included**

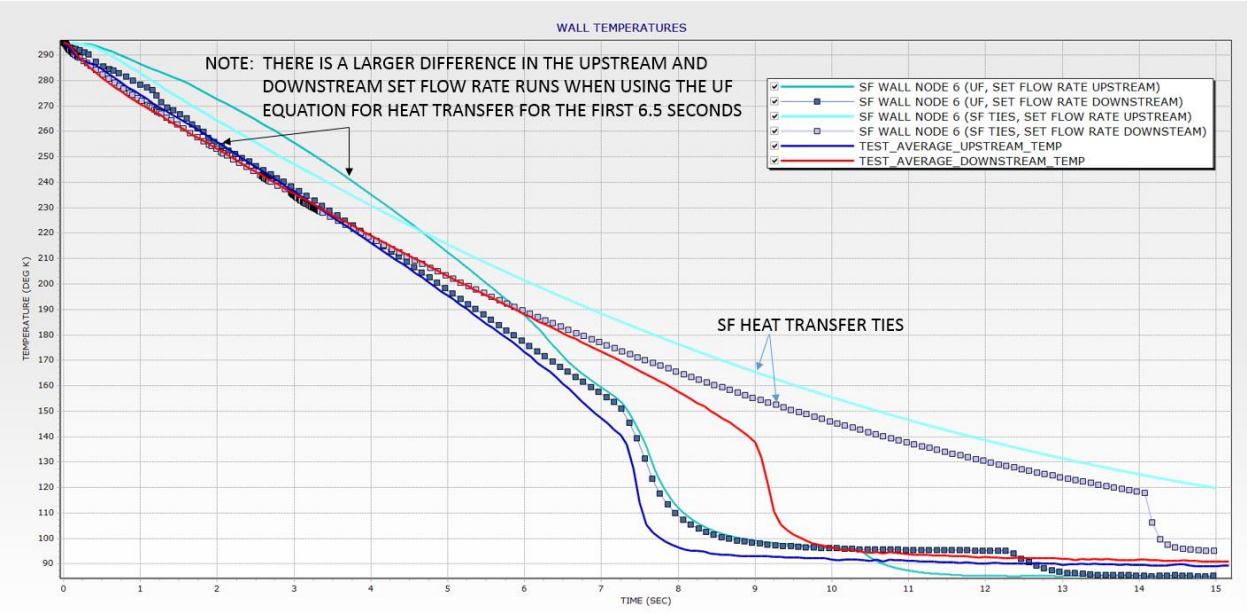

Figure 23: Vertical Upward Liquid Nitrogen Chill-down (29) UF and SF Heat Transfer Wall Temperature Results at Upstream Test Location

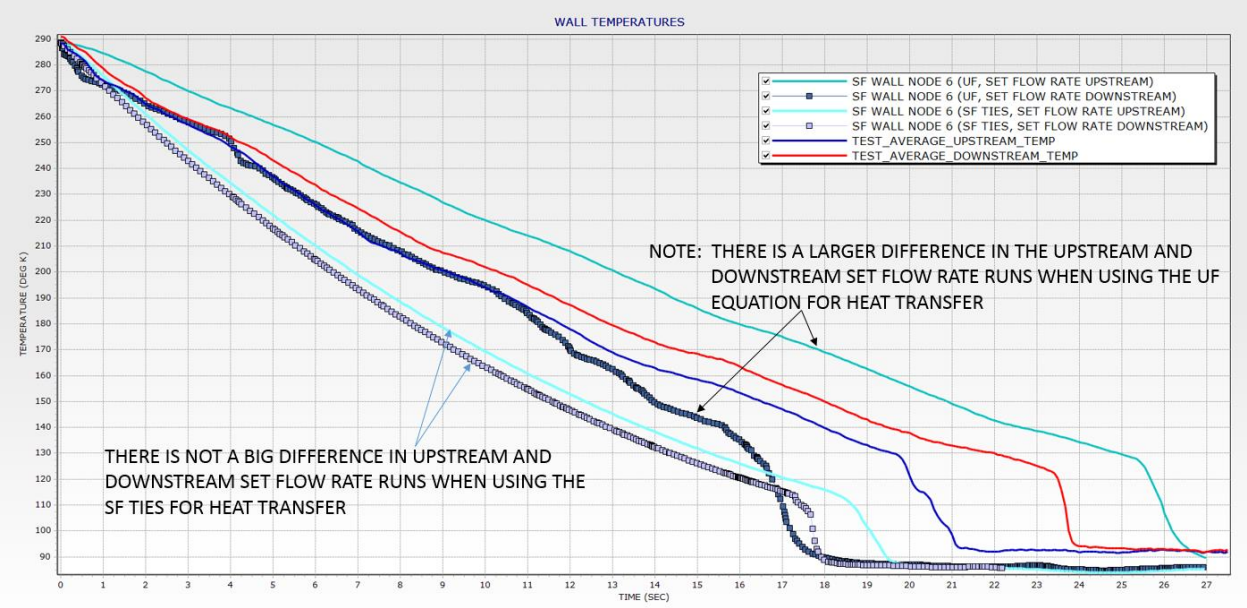

Figure 24: Vertical Upward Liquid Nitrogen Chill-down (12) UF and SF Heat Transfer Wall Temperature Results at Upstream Test Location

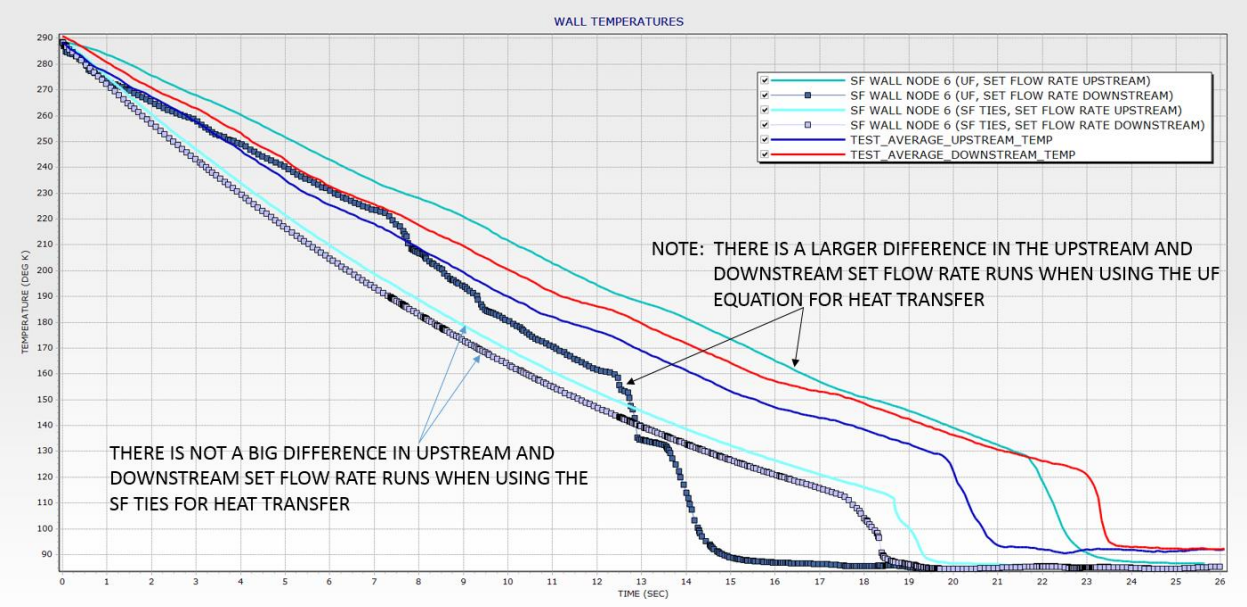

Figure 25: Vertical Upward Liquid Nitrogen Chill-down (25) UF and SF Heat Transfer Wall Temperature Results at Upstream Test Location

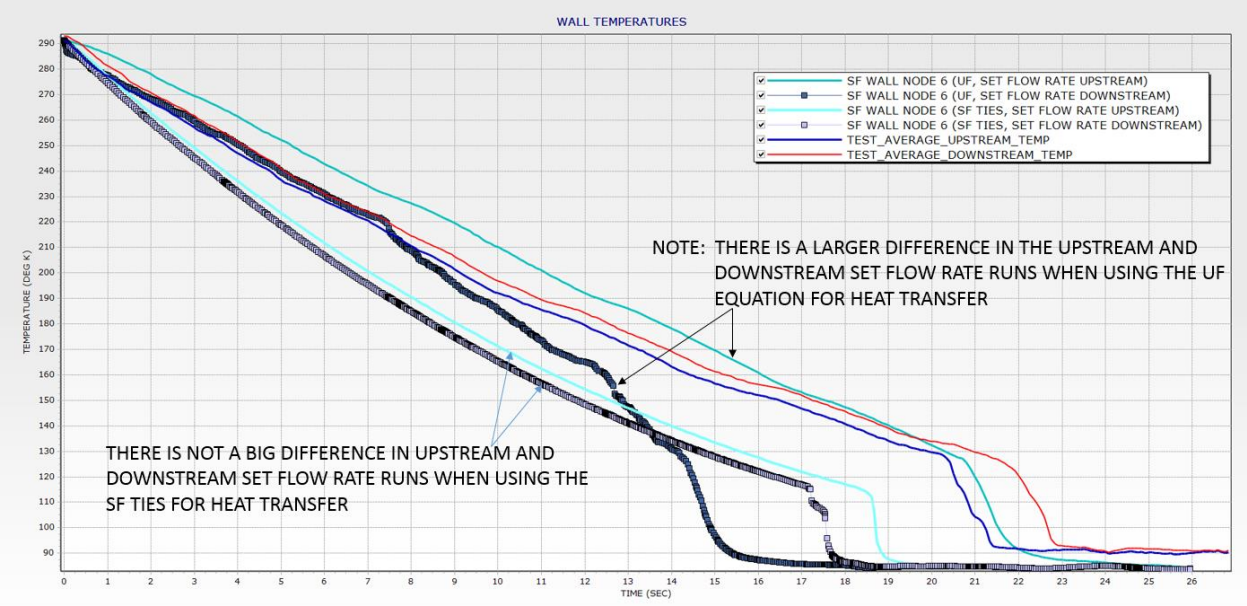

Figure 26: Vertical Upward Liquid Nitrogen Chill-down (2) UF and SF Heat Transfer Wall Temperature Results at Upstream Test Location

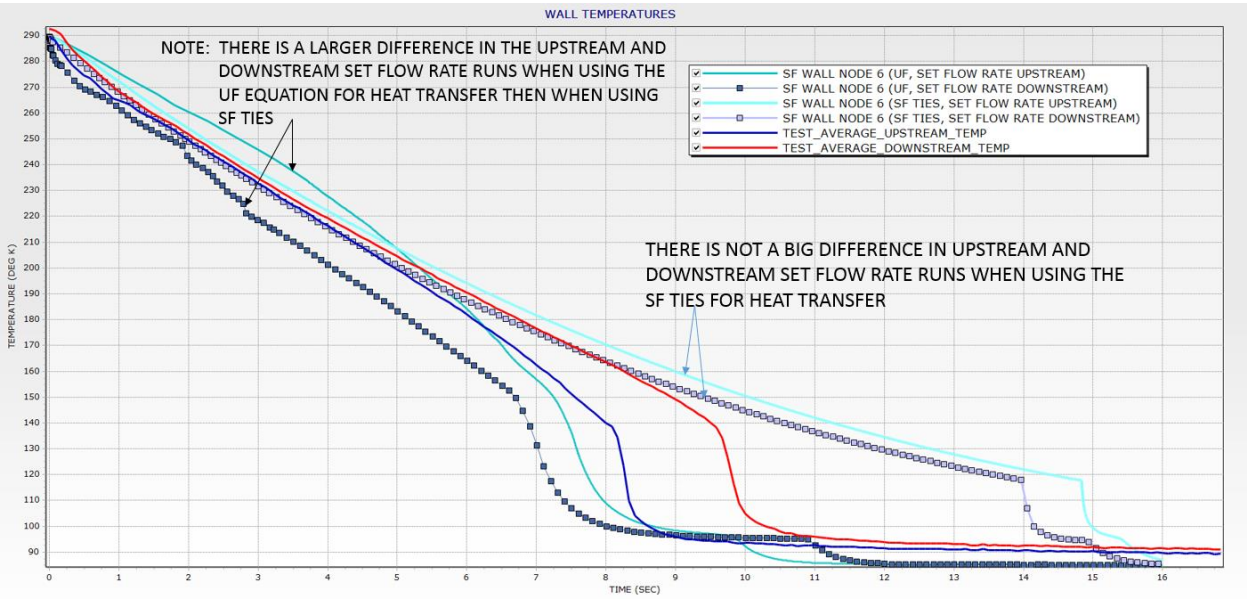

Figure 27: Vertical Upward Liquid Nitrogen Chill-down (39) UF and SF Heat Transfer Wall Temperature Results at Upstream Test Location

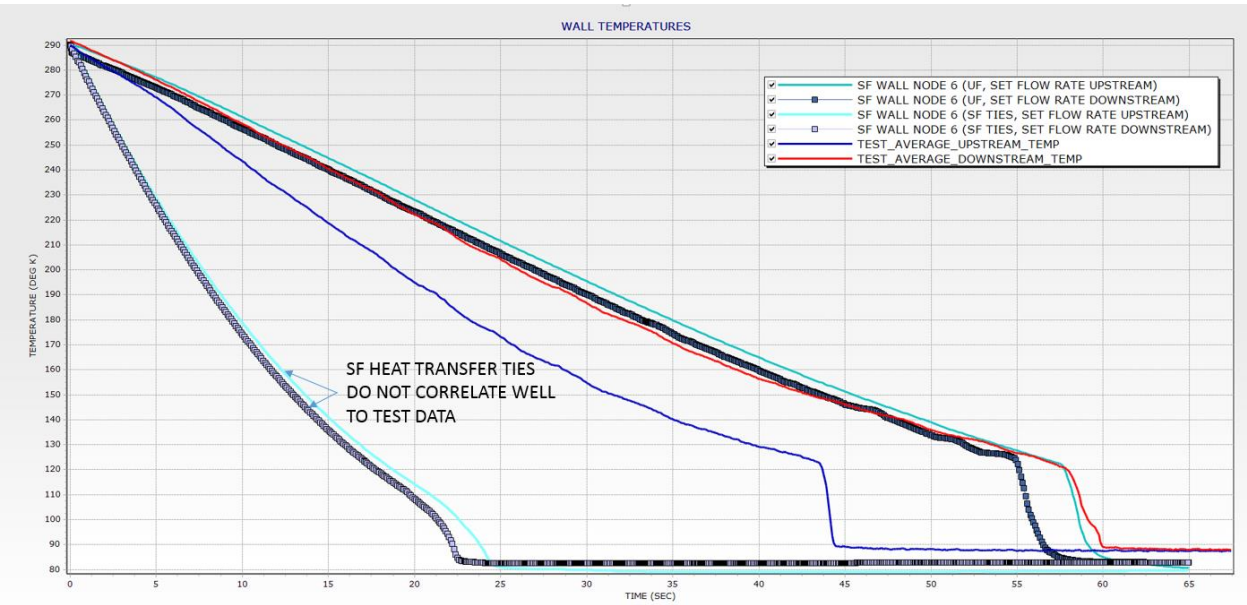

Figure 28: Vertical Upward Liquid Nitrogen Chill-down (50) UF and SF Heat Transfer Wall Temperature Results at Upstream Test Location

D. Liquid Hydrogen Chill-Down: Vertical Upward Flow

The cases for the liquid hydrogen chill-down include the Shah modification on the SF TIES (Equations 7a through 7c). Results varied across the board, meaning that the UF correlations, the SF TIES, and the SF TIES with Shah fared similarly in matching wall temperature test data. Sometimes a correlation fared slightly better but the others were still in an acceptable range of the test data.

The issue of test pressure data not correlating to the models, regardless the correlation being used, was also a problem as seen in the liquid nitrogen chill-down models. Figures 29a, 29b, 33a, and 33b show wall temperature results when an inlet pressure boundary was used instead of an inlet mass flow rate boundary. PT3 (see Figure 3) was used as the inlet pressure since this was available from test data, as well as PT5. All pressure boundary cases show a faster wall chill-down compared to test data. Figure 30 (refer to Figure 4 for SF LUMP identification) shows the corresponding flow rate obtained when PT3 was the inlet pressure using SF TIES with Shah. This flow rate is higher than the test data flow rate for the entire test chill-down time, causing increased heat transfer and thus the faster wall chill-down. Although the pressures (PT3 and SF calculated inlet pressure at LUMP 2) eventually come to relative agreement, there is some discrepancy for the first several seconds using the SF TIES with Shah.

Figure 29c shows the wall temperature results at the sight glass location. The material properties used at the sight glass location were that of Pyrex. For all correlations the model does not correlate to test data very well.

Figure 31a through 31b show the void fractions and qualities for the upstream test location and the sight glass.

A test case was run with the pipe wall radially discretized with ten nodes. The wall temperature results are shown in Figure 32a and 32b using SF TIES with the Shah modification. The results include the inner and outer wall temperatures compared to the case where there was no radial wall discretization. Radial wall discretization did not provide significant changes in wall chill-down temperature profiles or chill-down time.

Figures 33 through 46 show wall temperature results for the various liquid hydrogen chill-down test cases using the UF correlations, SF TIES, and SF TIES with the Shah modification. Also included in these figures are the void fraction and quality for the upstream test location and sight glass.

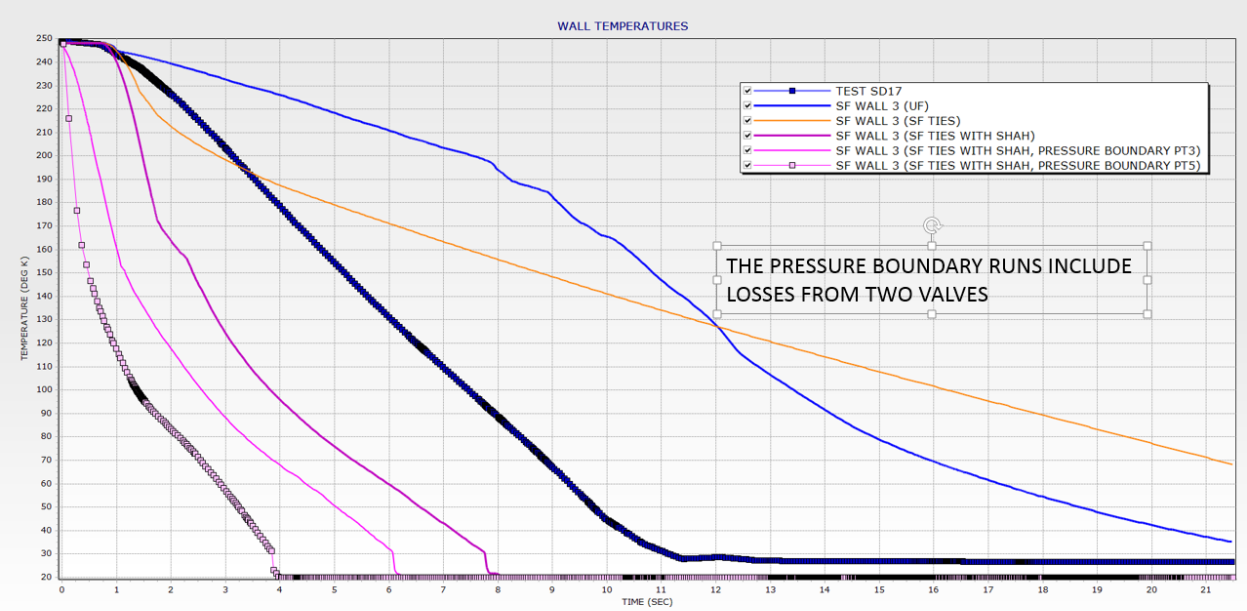

Figure 29a: Vertical Upward Liquid Hydrogen Chill-down (3b) UF and SF Heat Transfer Wall Temperature Results at Upstream Test Location (Includes Shah Modification for SF TIES, and Pressure Inlet and Outlet Boundary)

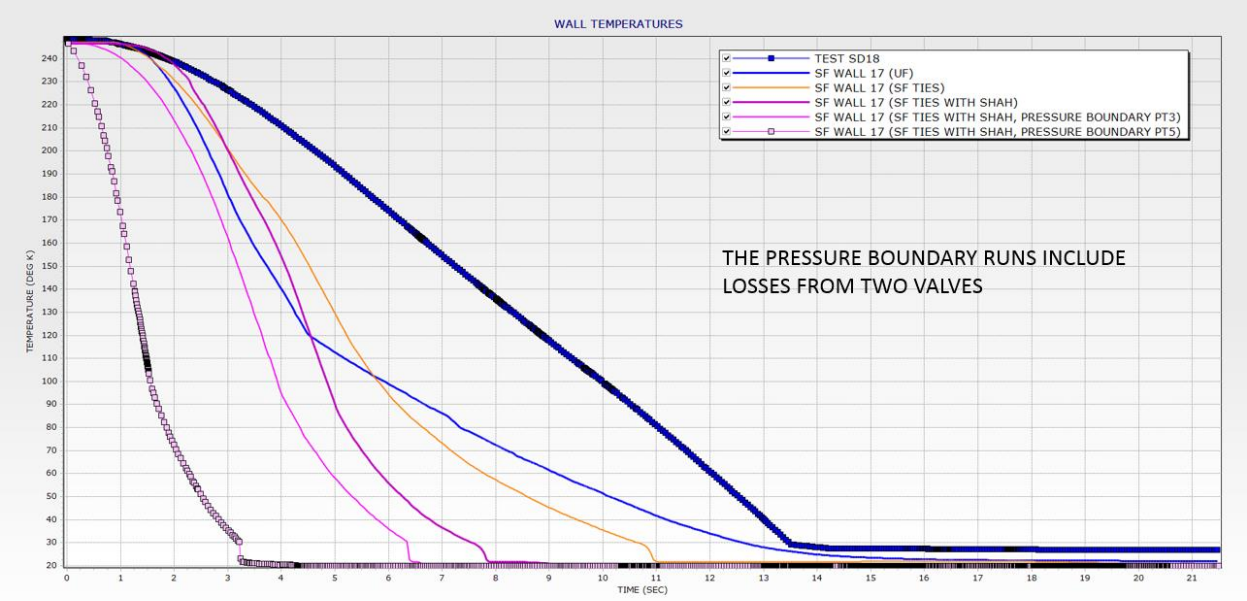

Figure 29b: Vertical Upward Liquid Hydrogen Chill-down (3b) UF and SF Heat Transfer Wall Temperature Results at Downstream Test Location (Includes Shah Modification for SF TIES, and Pressure Inlet and Outlet Boundary)

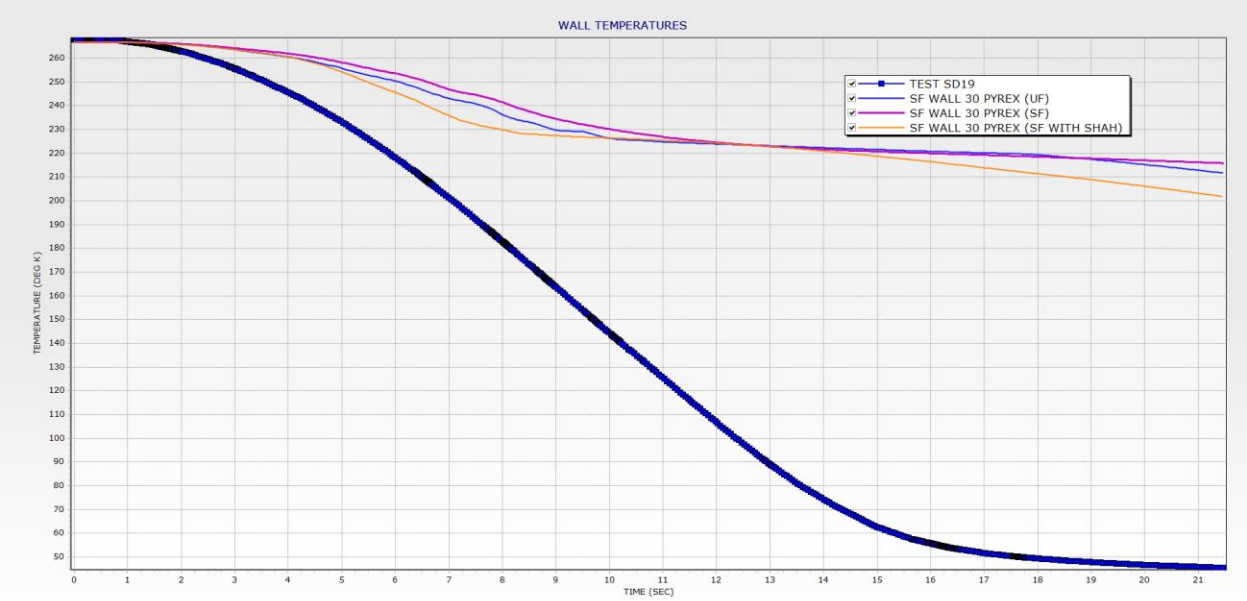

Figure 29c: Vertical Upward Liquid Hydrogen Chill-down (3b) UF and SF Heat Transfer Wall Temperature Results at Sight Glass Test Location (Includes Shah Modification for SF TIES, and Pressure Inlet and Outlet Boundary)

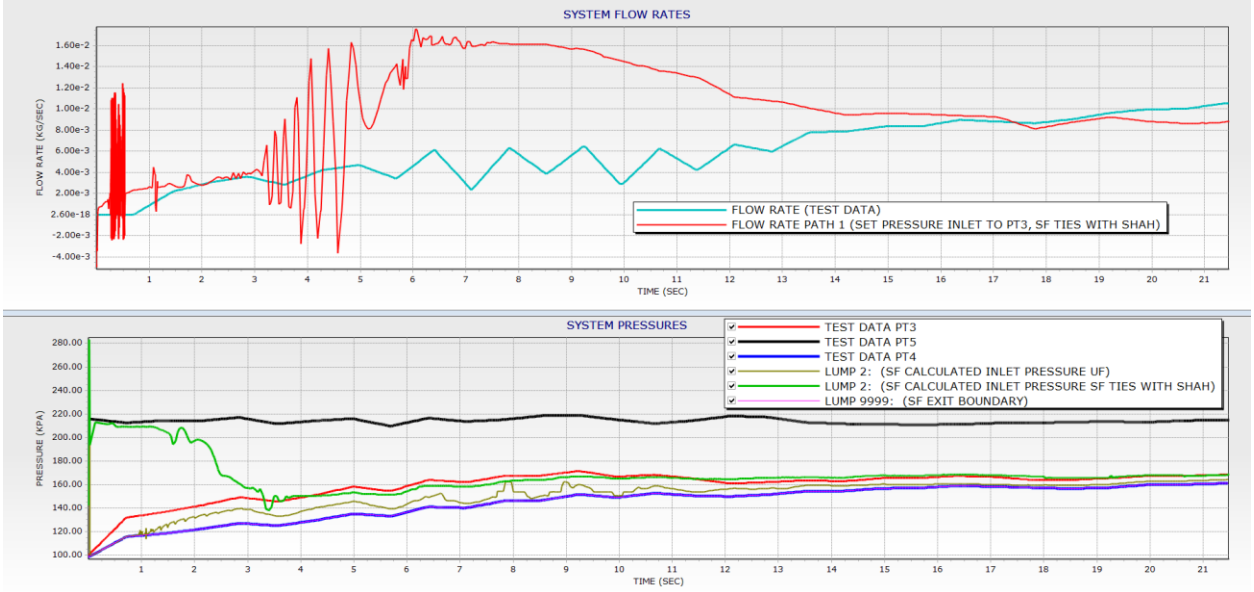

Figure 30: Vertical Upward Liquid Hydrogen Chill-down (3b) UF and SF with Shah Heat Transfer Flow Rate and Pressure Results (Includes Pressure Inlet and Outlet Boundary)

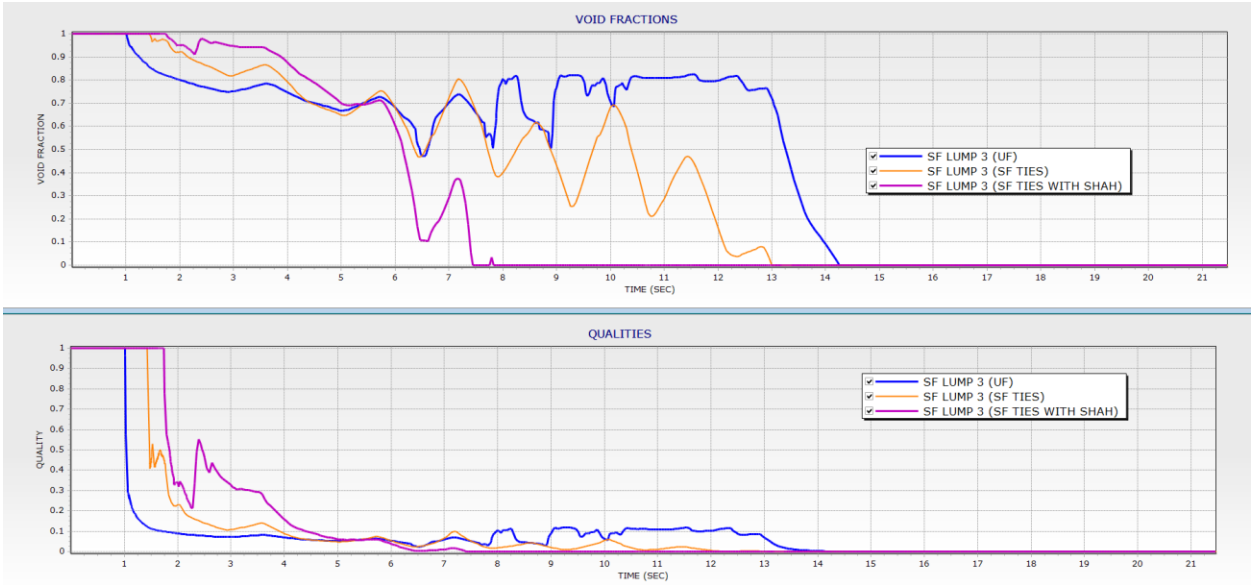

Figure 31a: Vertical Upward Liquid Hydrogen Chill-down (3b) UF and SF Heat Transfer Void Fraction and Quality Results at Upstream Test Location (Includes Shah Modification for SF TIES)

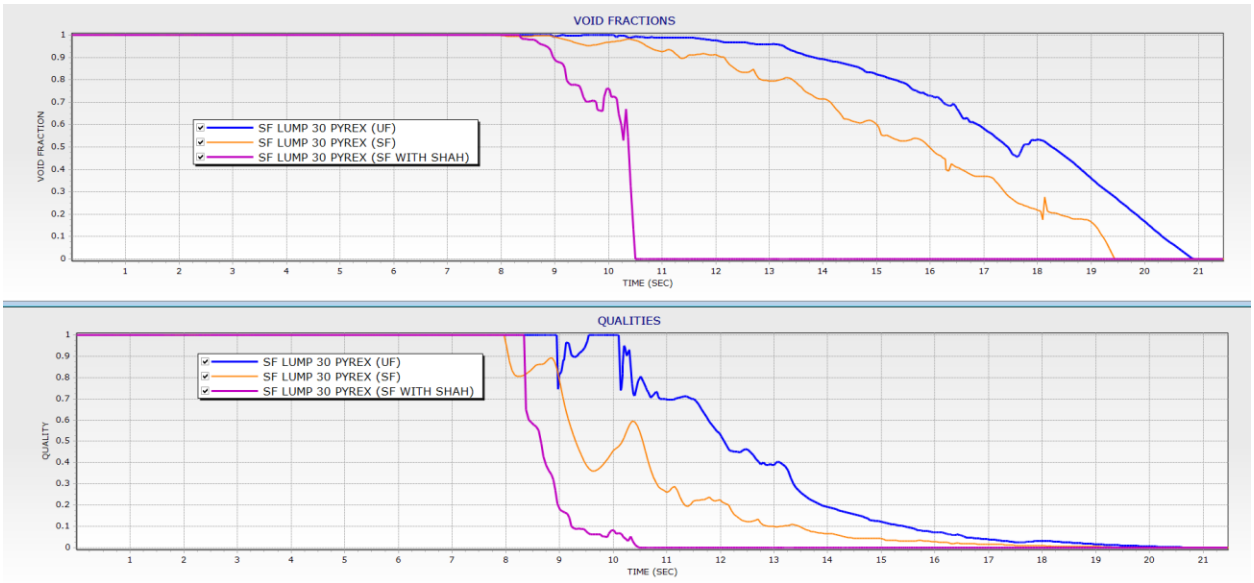

Figure 31b: Vertical Upward Liquid Hydrogen Chill-down (3b) UF and SF Heat Transfer Void Fraction and Quality Results at Sight Glass Test Location (Includes Shah Modification for SF TIES)

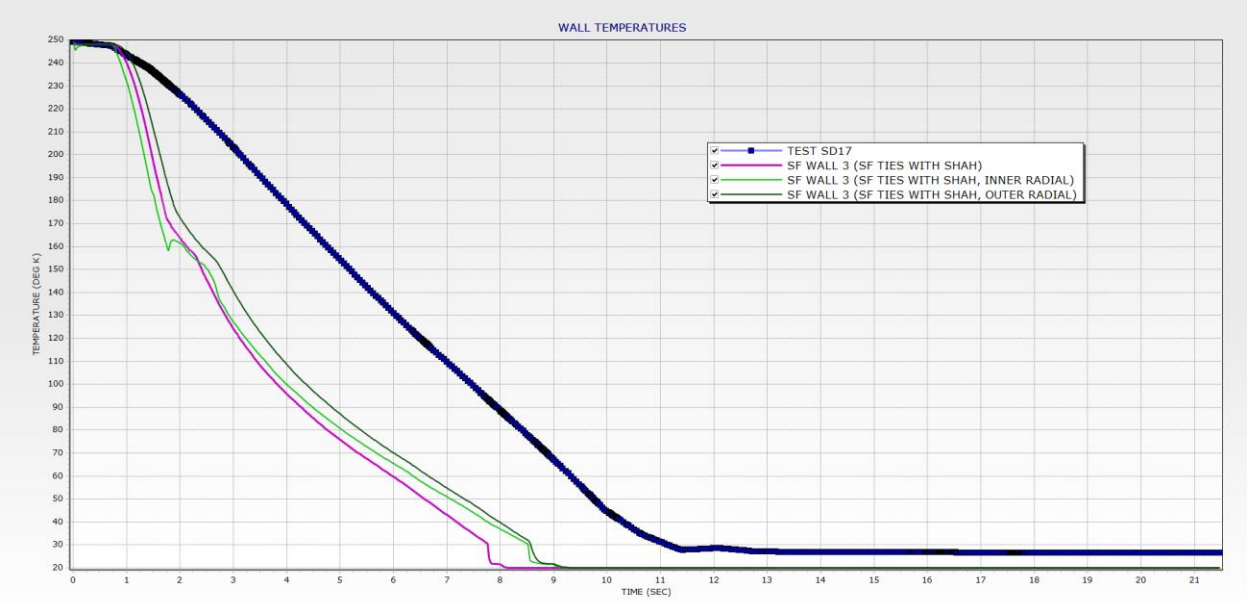

Figure 32a: Vertical Upward Liquid Hydrogen Chill-down (3b) SF Heat Transfer Inner and Outer Wall Temperature Results at Upstream Test Location (Includes Shah Modification for SF TIES)

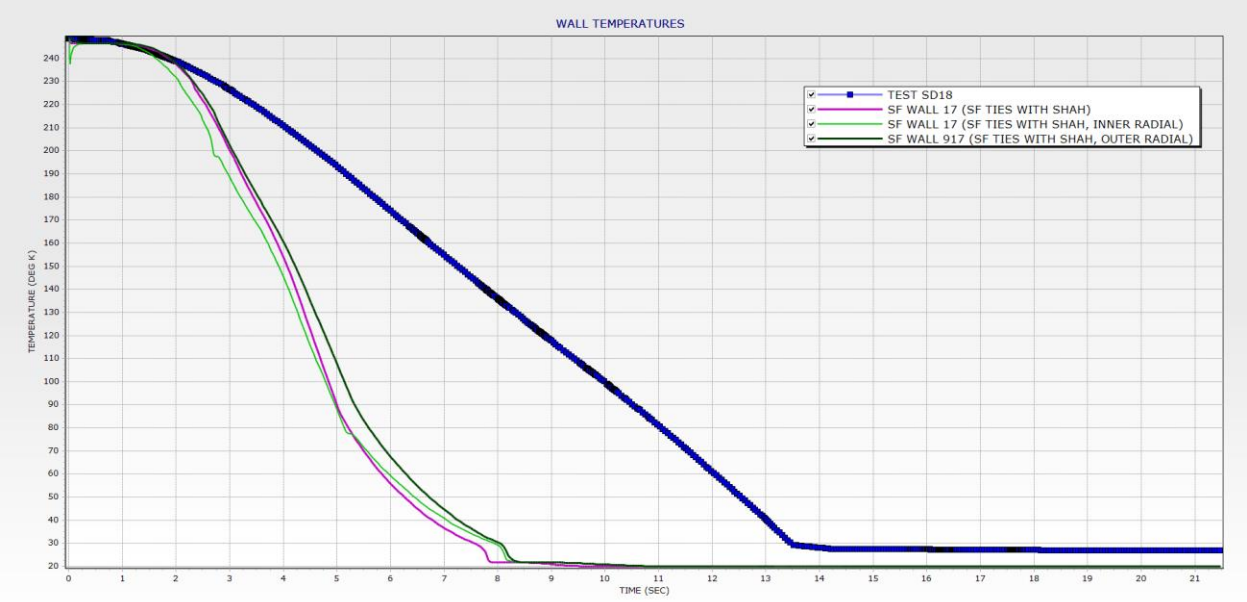

Figure 32b: Vertical Upward Liquid Hydrogen Chill-down (3b) SF Heat Transfer Inner and Outer Wall Temperature Results at Downstream Test Location (Includes Shah Modification for SF TIES)

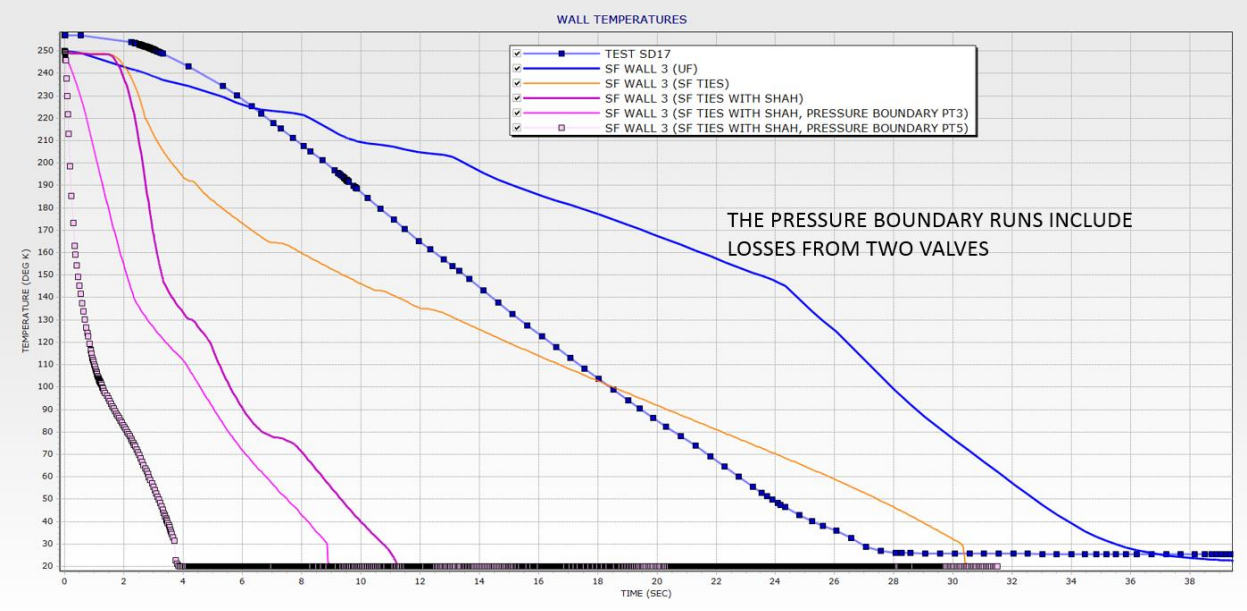

Figure 33a: Vertical Upward Liquid Hydrogen Chill-down (1b) UF and SF Heat Transfer Wall Temperature Results at Upstream Test Location (Includes Shah Modification for SF TIES, and Pressure Inlet and Outlet Boundary)

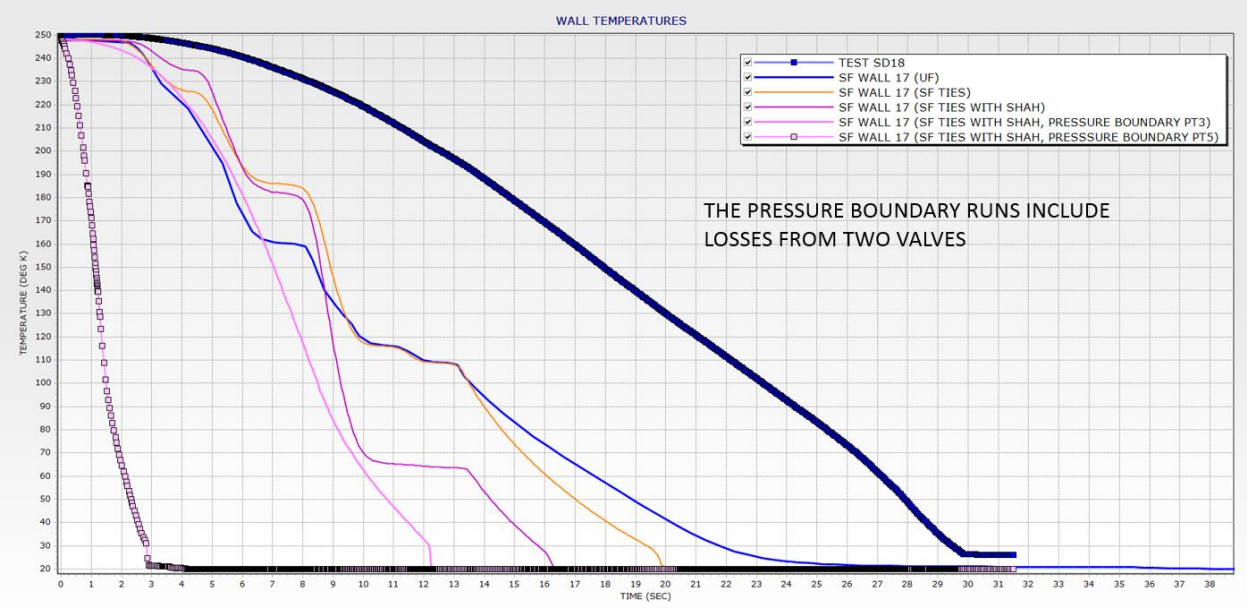

Figure 33b: Vertical Upward Liquid Hydrogen Chill-down (1b) UF and SF Heat Transfer Wall Temperature Results at Downstream Test Location (Includes Shah Modification for SF TIES, and Pressure Inlet and Outlet Boundary)

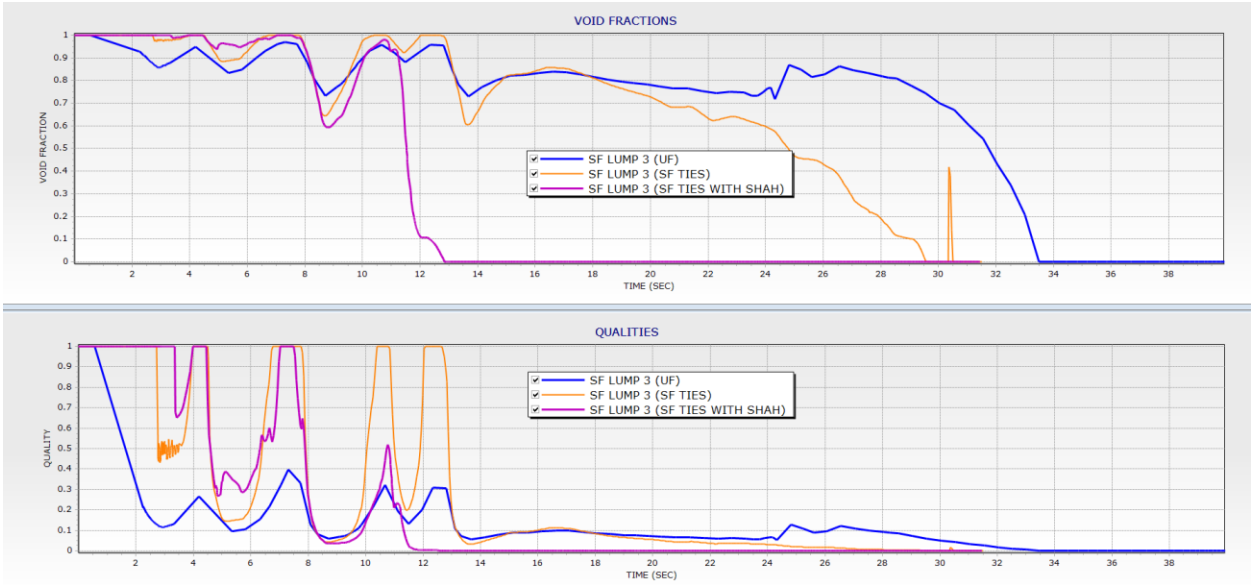

Figure 34a: Vertical Upward Liquid Hydrogen Chill-down (1b) UF and SF Heat Transfer Void Fraction and Quality Results at Upstream Test Location (Includes Shah Modification for SF TIES)

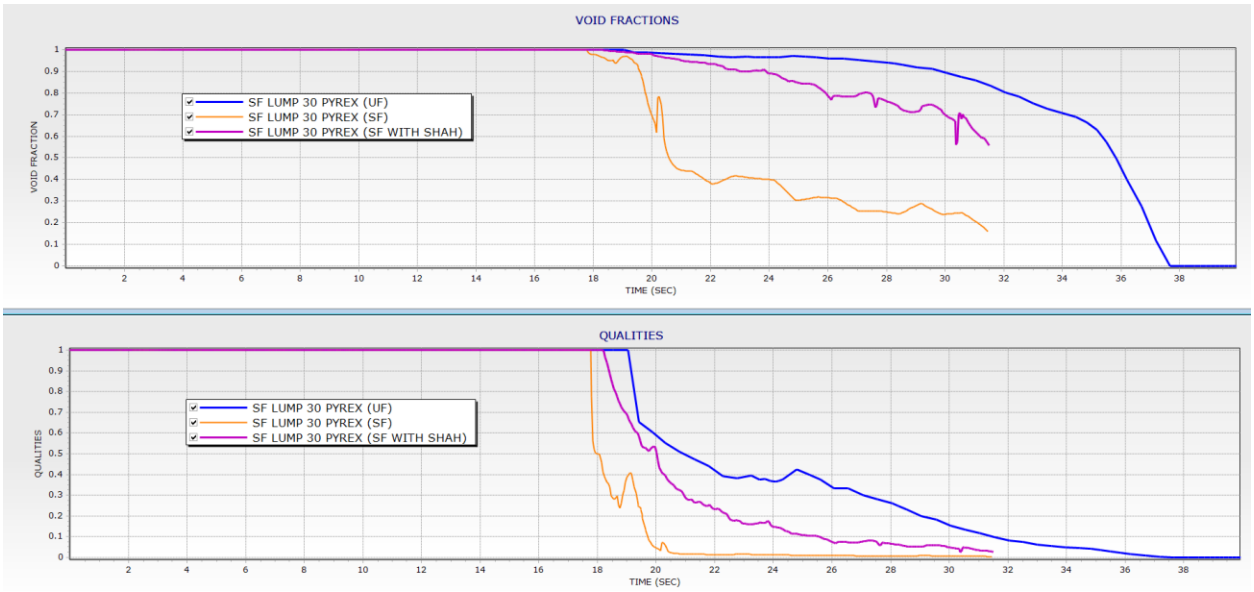

Figure 34b: Vertical Upward Liquid Hydrogen Chill-down (1b) UF and SF Heat Transfer Void Fraction and Quality Results at Sight Glass Test Location (Includes Shah Modification for SF TIES)

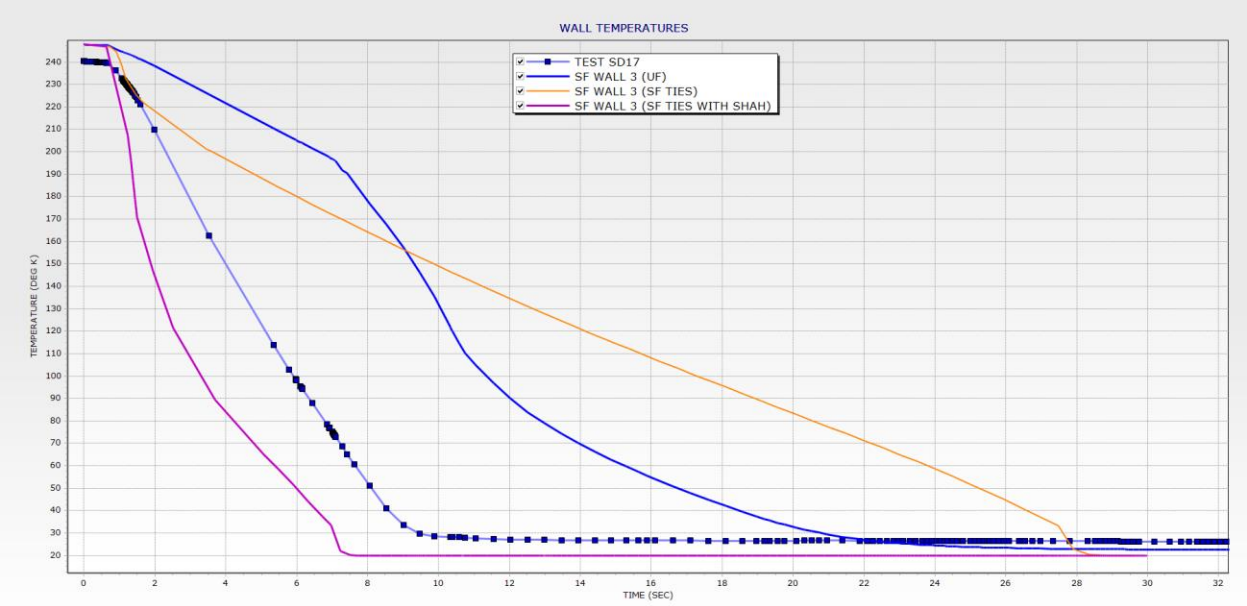

Figure 35a: Vertical Upward Liquid Hydrogen Chill-down (7b) UF and SF Heat Transfer Wall Temperature Results at Upstream Test Location (Includes Shah Modification for SF TIES)

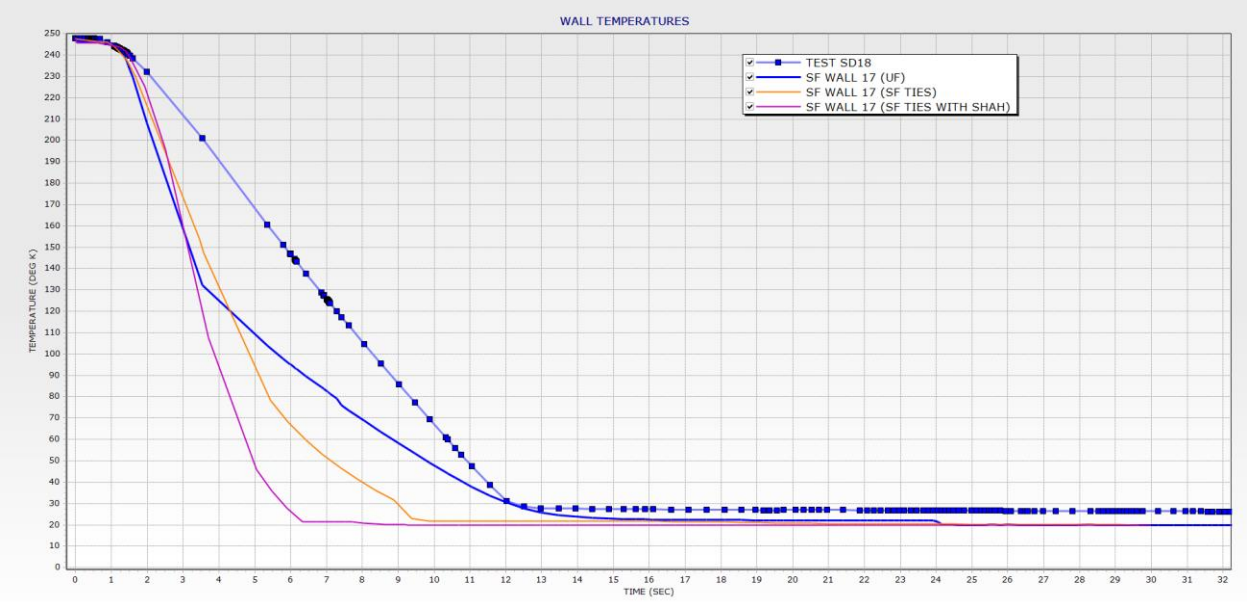

Figure 35b: Vertical Upward Liquid Hydrogen Chill-down (7b) UF and SF Heat Transfer Wall Temperature Results at Downstream Test Location (Includes Shah Modification for SF TIES)

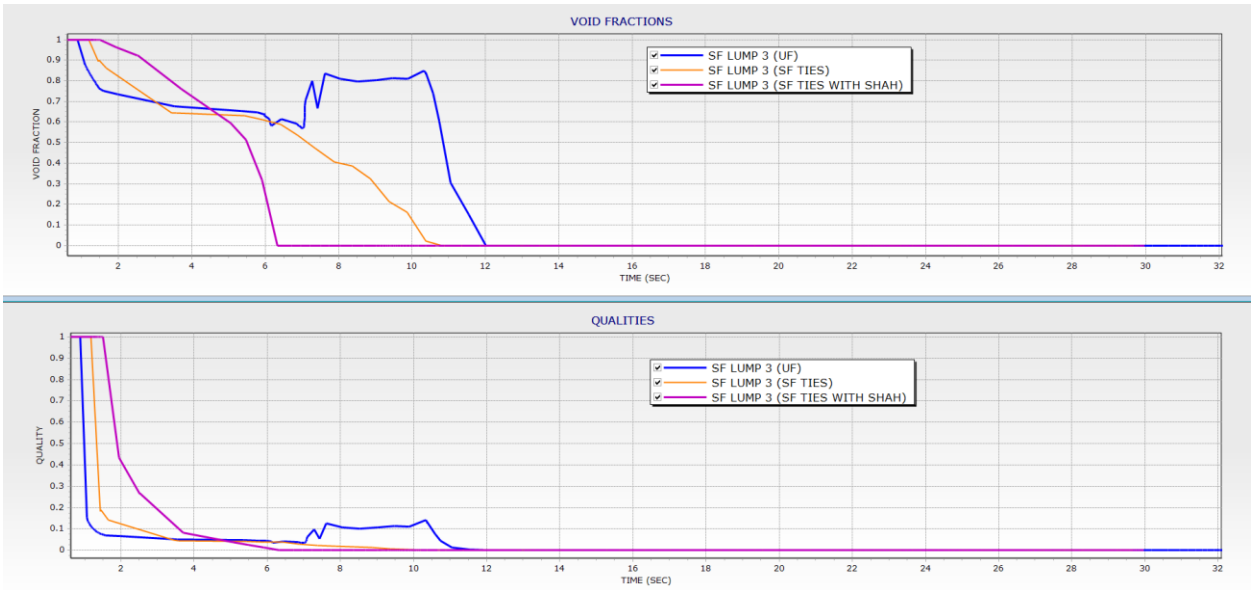

Figure 36a: Vertical Upward Liquid Hydrogen Chill-down (7b) UF and SF Heat Transfer Void Fraction and Quality Results at Upstream Test Location (Includes Shah Modification for SF TIES)

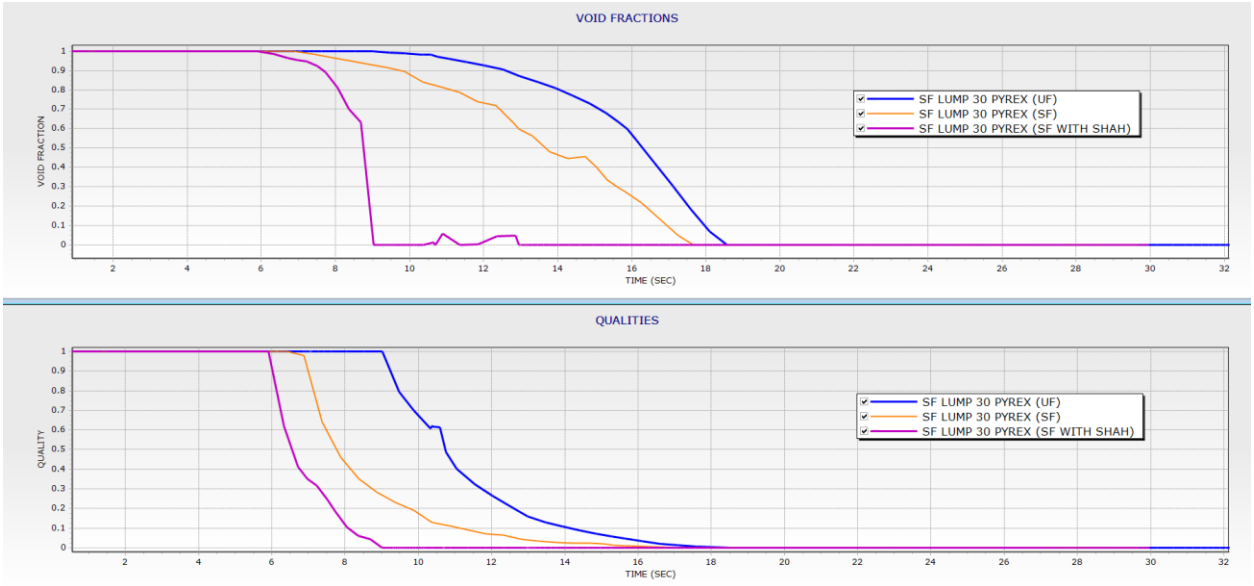

Figure 36b: Vertical Upward Liquid Hydrogen Chill-down (7b) UF and SF Heat Transfer Void Fraction and Quality Results at Sight Glass Test Location (Includes Shah Modification for SF TIES)

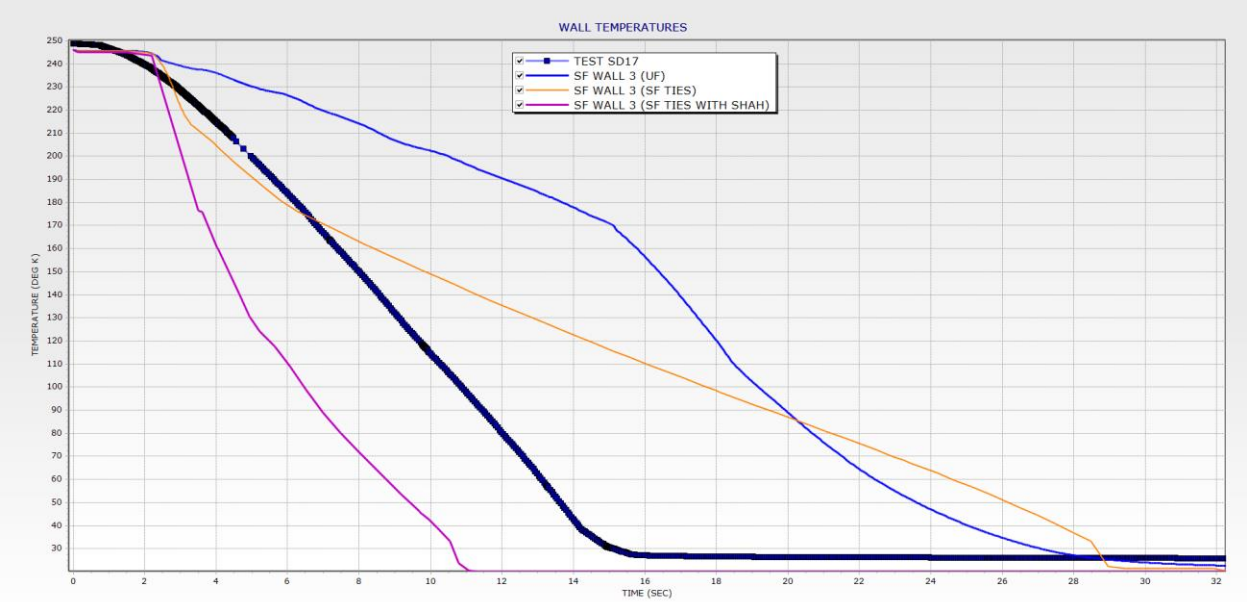

Figure 37a: Vertical Upward Liquid Hydrogen Chill-down (12b) UF and SF Heat Transfer Wall Temperature Results at Upstream Test Location (Includes Shah Modification for SF TIES)

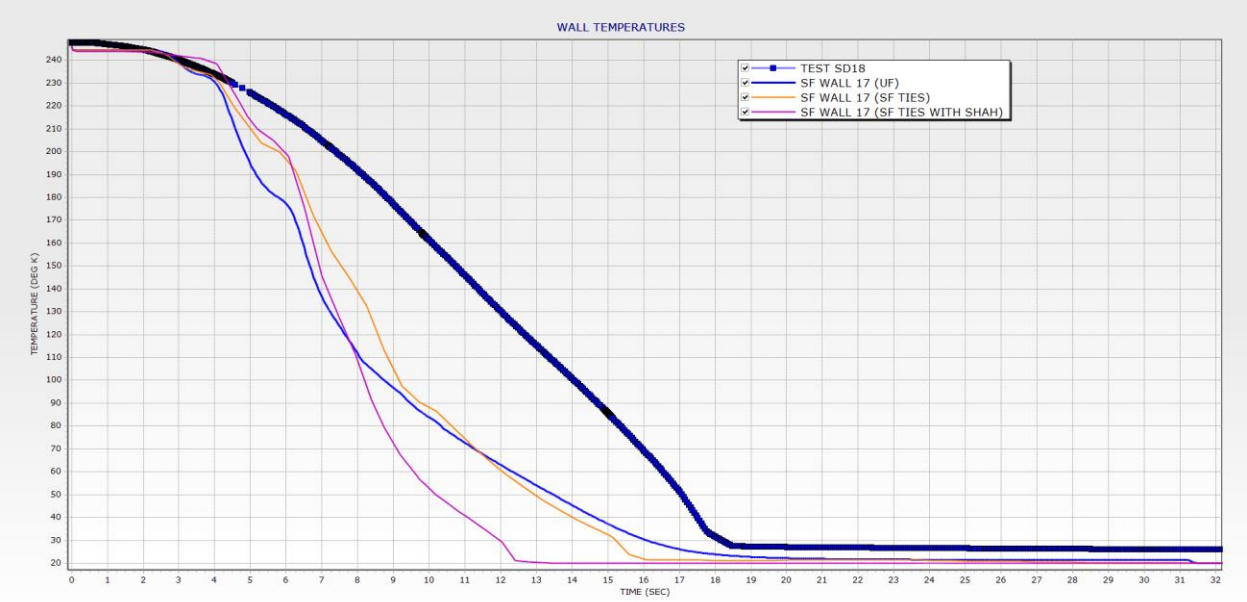

Figure 37b: Vertical Upward Liquid Hydrogen Chill-down (12b) UF and SF Heat Transfer Wall Temperature Results at Downstream Test Location (Includes Shah Modification for SF TIES)

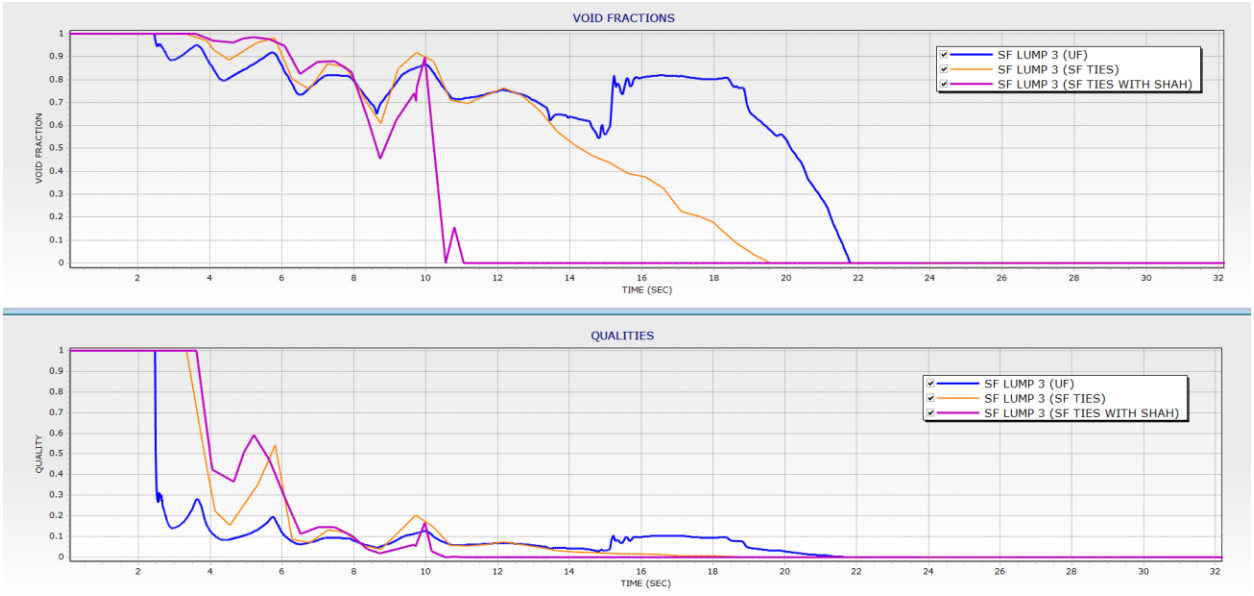

Figure 38a: Vertical Upward Liquid Hydrogen Chill-down (7b) UF and SF Heat Transfer Void Fraction and Quality Results at Upstream Test Location (Includes Shah Modification for SF TIES)

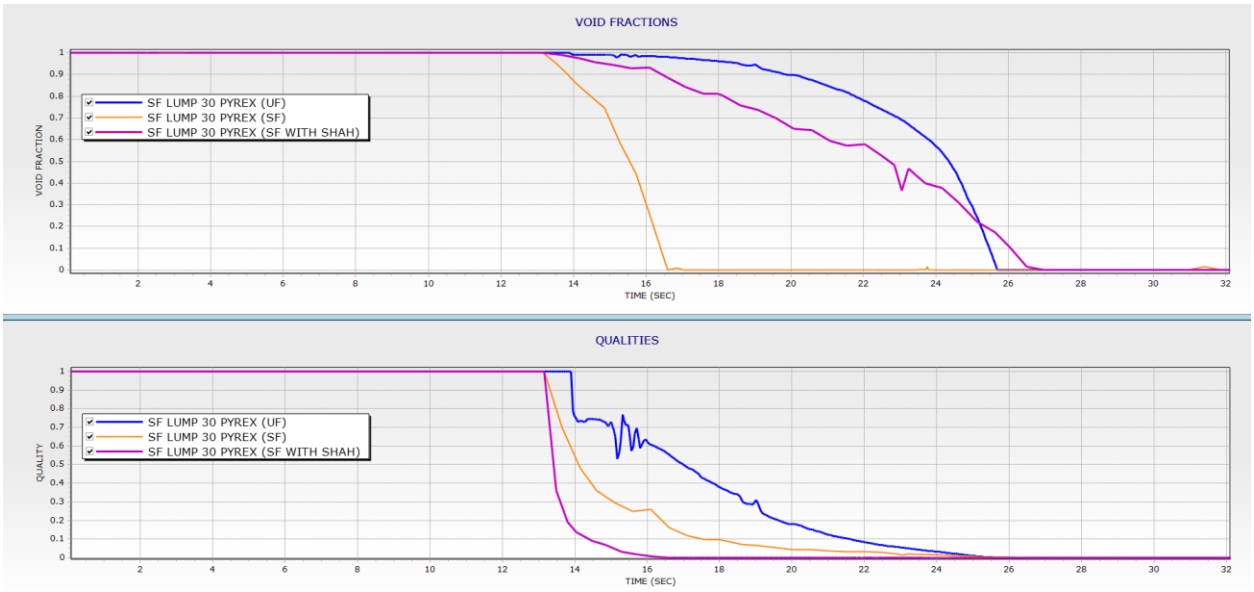

Figure 38b: Vertical Upward Liquid Hydrogen Chill-down (7b) UF and SF Heat Transfer Void Fraction and Quality Results at Sight Glass Test Location (Includes Shah Modification for SF TIES)

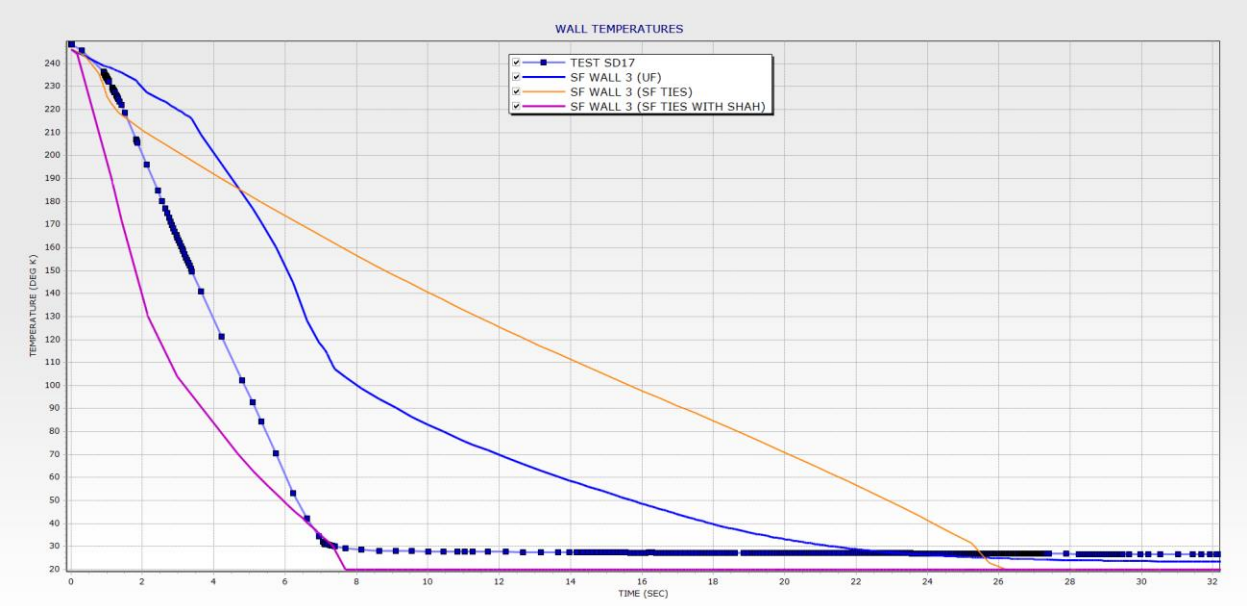

Figure 39a: Vertical Upward Liquid Hydrogen Chill-down (15b) UF and SF Heat Transfer Wall Temperature Results at Upstream Test Location (Includes Shah Modification for SF TIES)

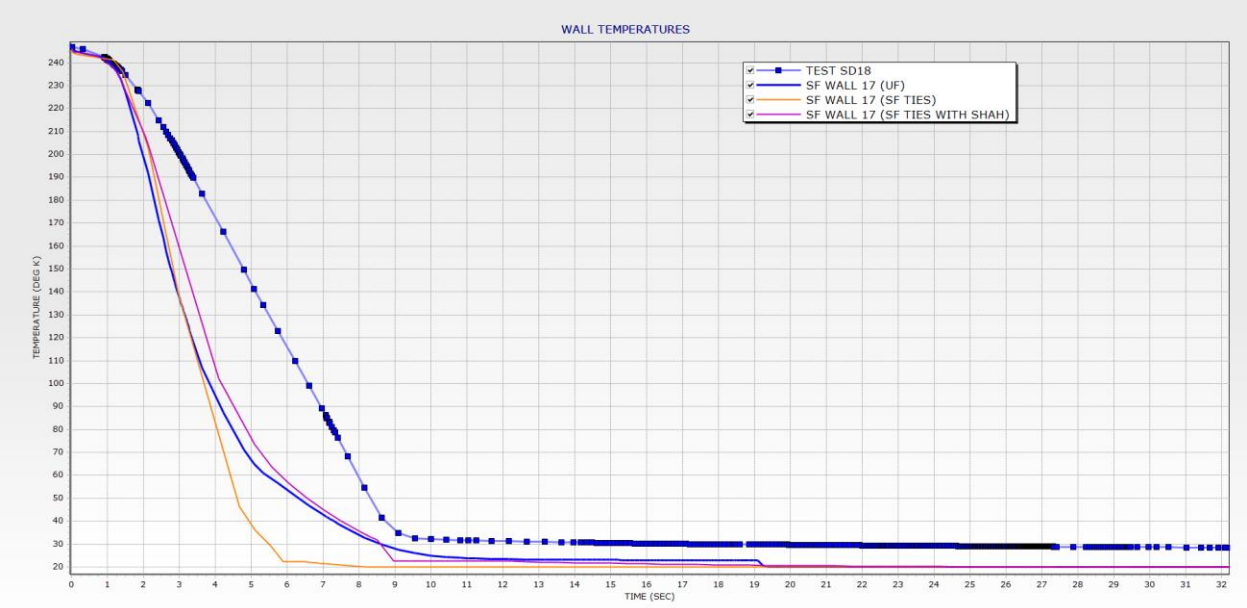

Figure 39b: Vertical Upward Liquid Hydrogen Chill-down (15b) UF and SF Heat Transfer Wall Temperature Results at Downstream Test Location (Includes Shah Modification for SF TIES)

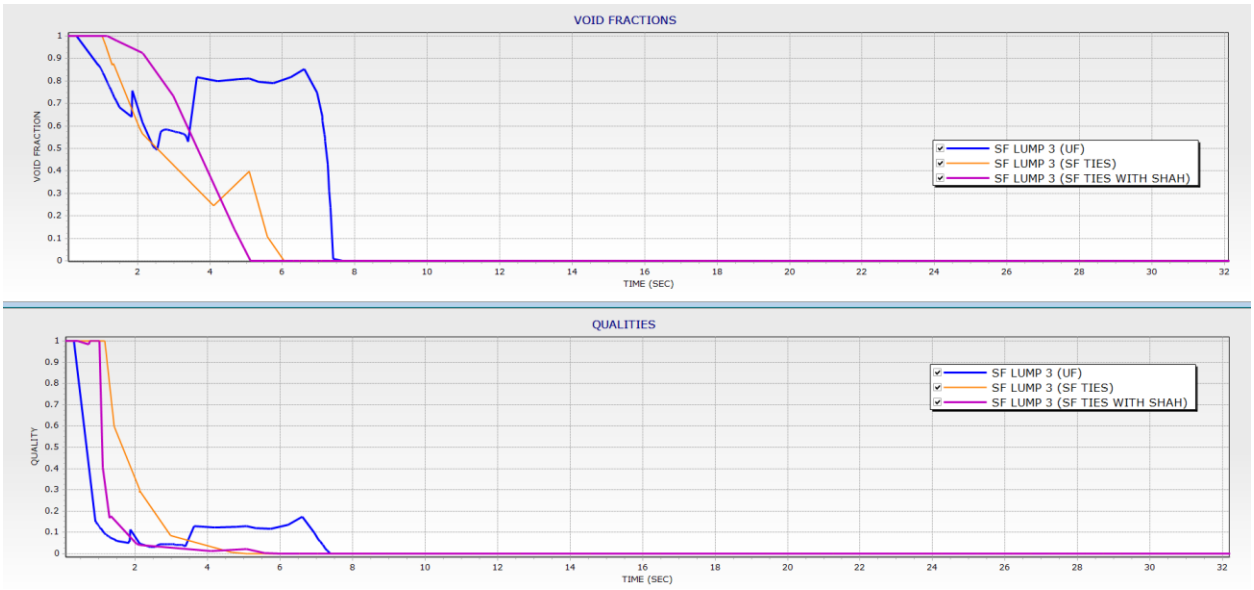

Figure 40a: Vertical Upward Liquid Hydrogen Chill-down (12b) UF and SF Heat Transfer Void Fraction and Quality Results at Upstream Test Location (Includes Shah Modification for SF TIES)

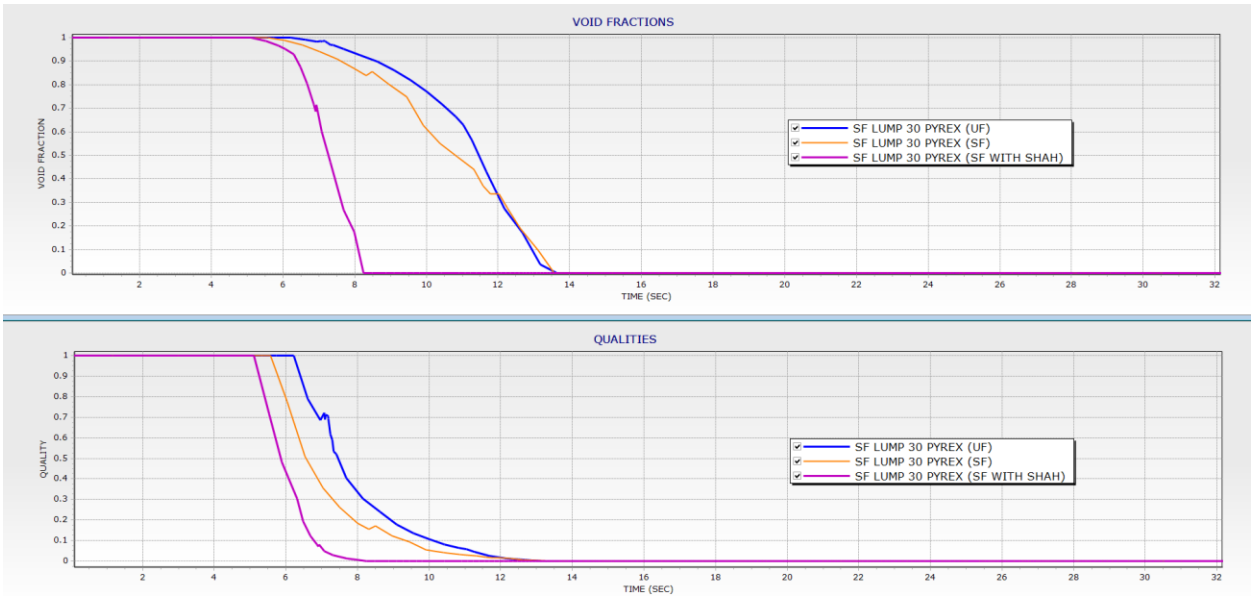

Figure 40b: Vertical Upward Liquid Hydrogen Chill-down (12b) UF and SF Heat Transfer Void Fraction and Quality Results at Sight Glass Test Location (Includes Shah Modification for SF TIES)

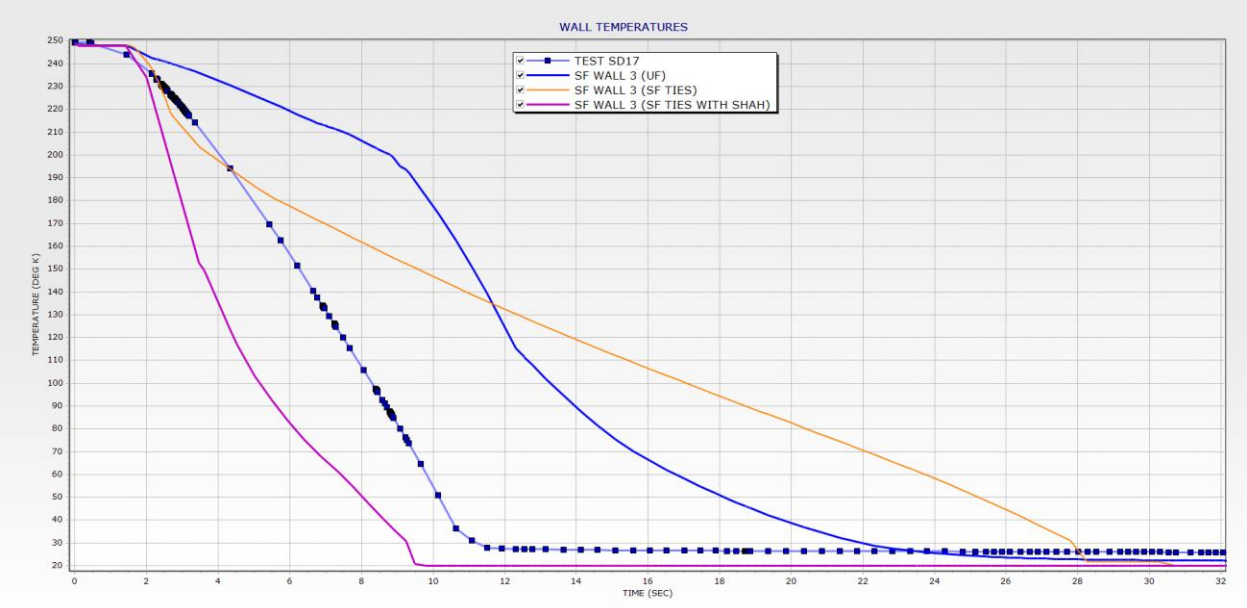

Figure 41a: Vertical Upward Liquid Hydrogen Chill-down (6b) UF and SF Heat Transfer Wall Temperature Results at Upstream Test Location (Includes Shah Modification for SF TIES)

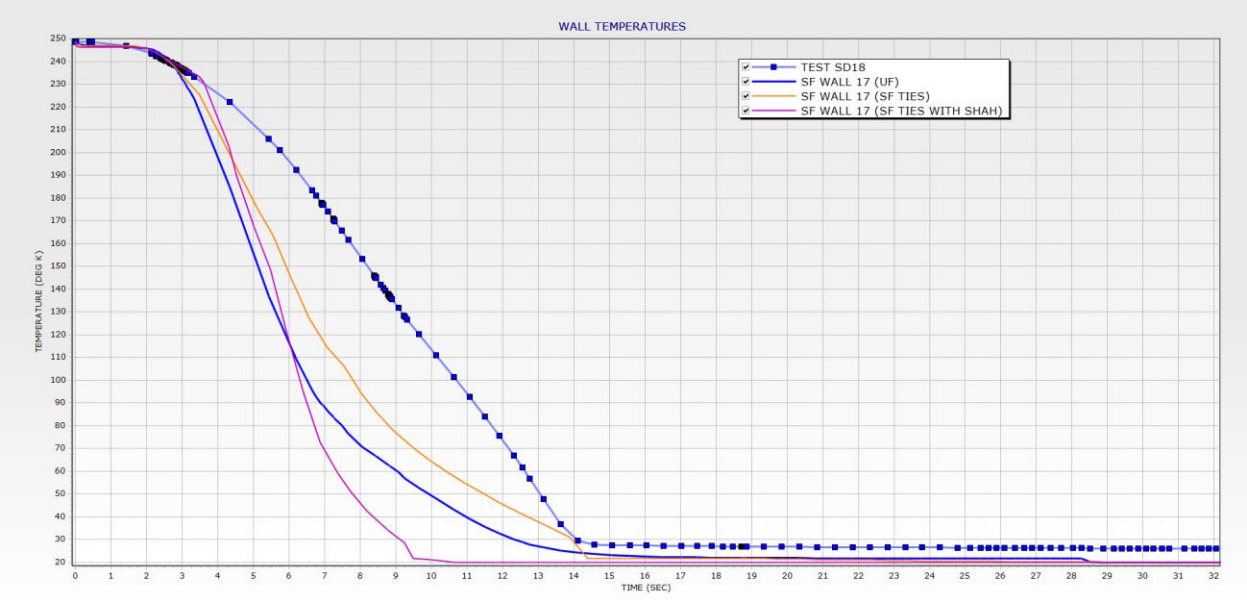

Figure 41b: Vertical Upward Liquid Hydrogen Chill-down (6b) UF and SF Heat Transfer Wall Temperature Results at Downstream Test Location (Includes Shah Modification for SF TIES)

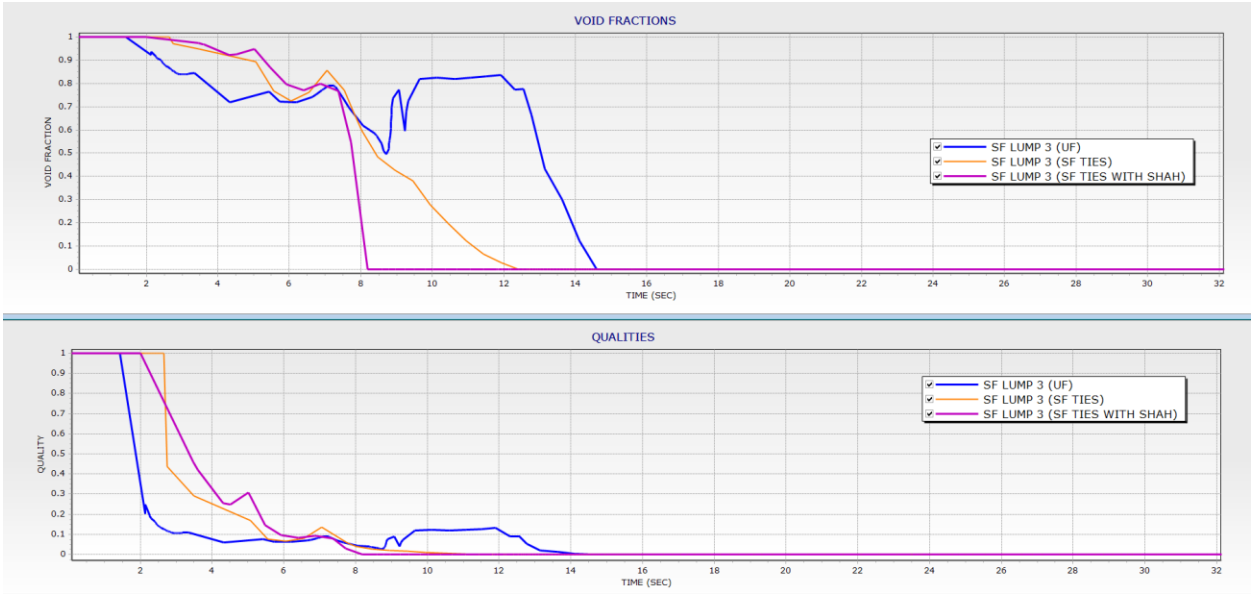

Figure 42a: Vertical Upward Liquid Hydrogen Chill-down (6b) UF and SF Heat Transfer Void Fraction and Quality Results at Upstream Test Location (Includes Shah Modification for SF TIES)

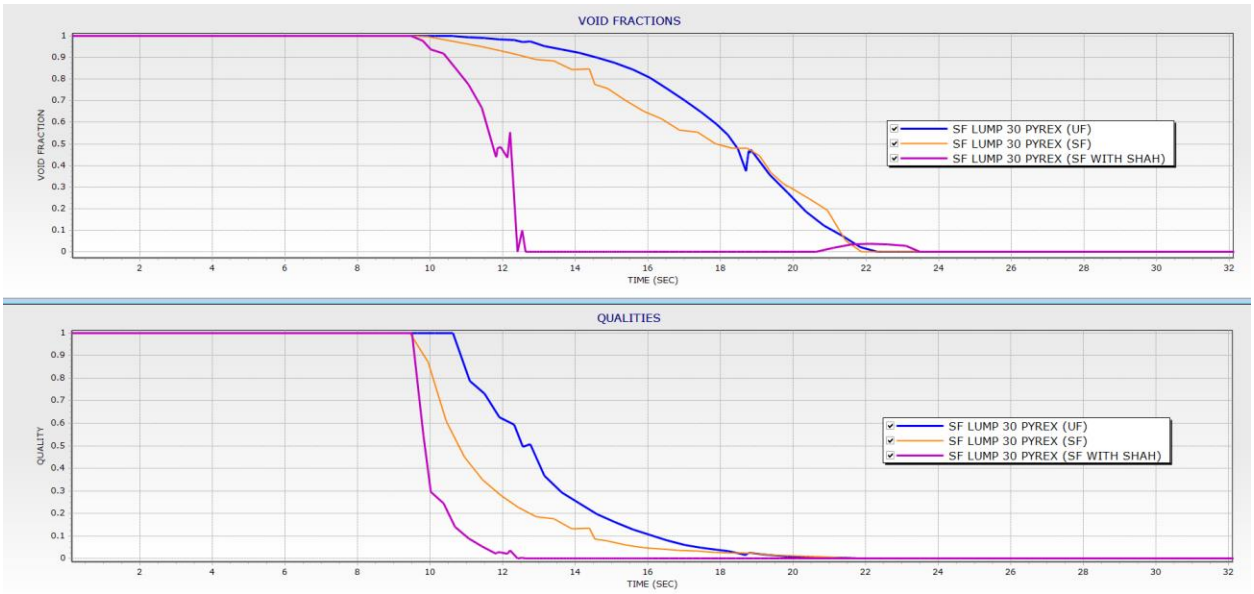

Figure 42b: Vertical Upward Liquid Hydrogen Chill-down (6b) UF and SF Heat Transfer Void Fraction and Quality Results at Sight Glass Test Location (Includes Shah Modification for SF TIES)

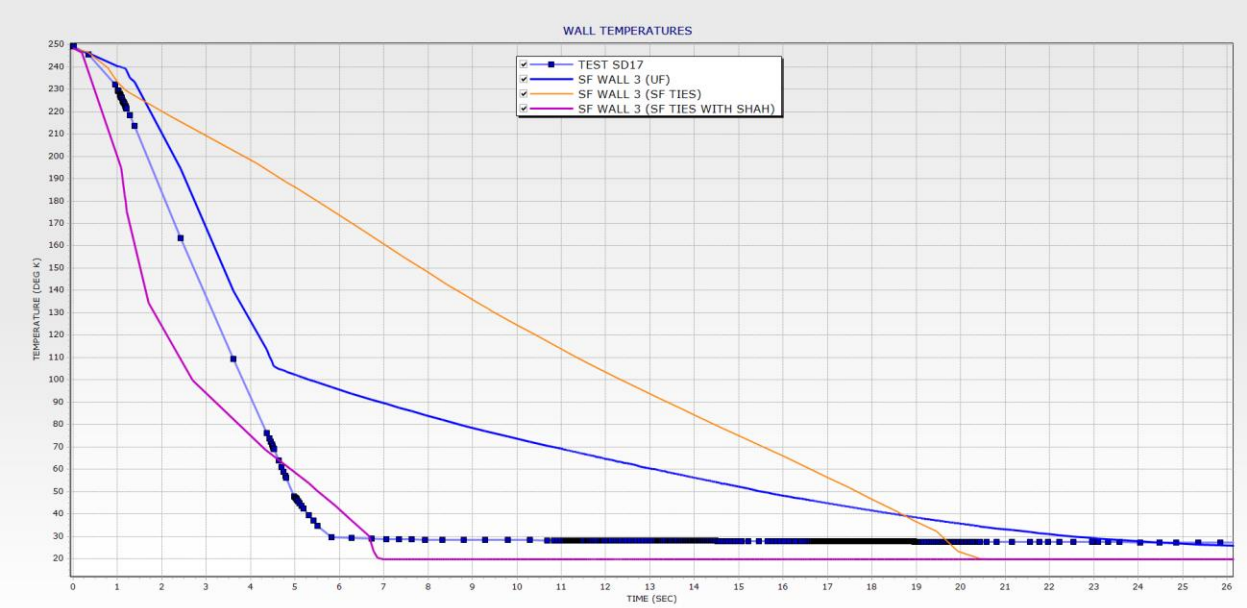

Figure 43a: Vertical Upward Liquid Hydrogen Chill-down (8b) UF and SF Heat Transfer Wall Temperature Results at Upstream Test Location (Includes Shah Modification for SF TIES)

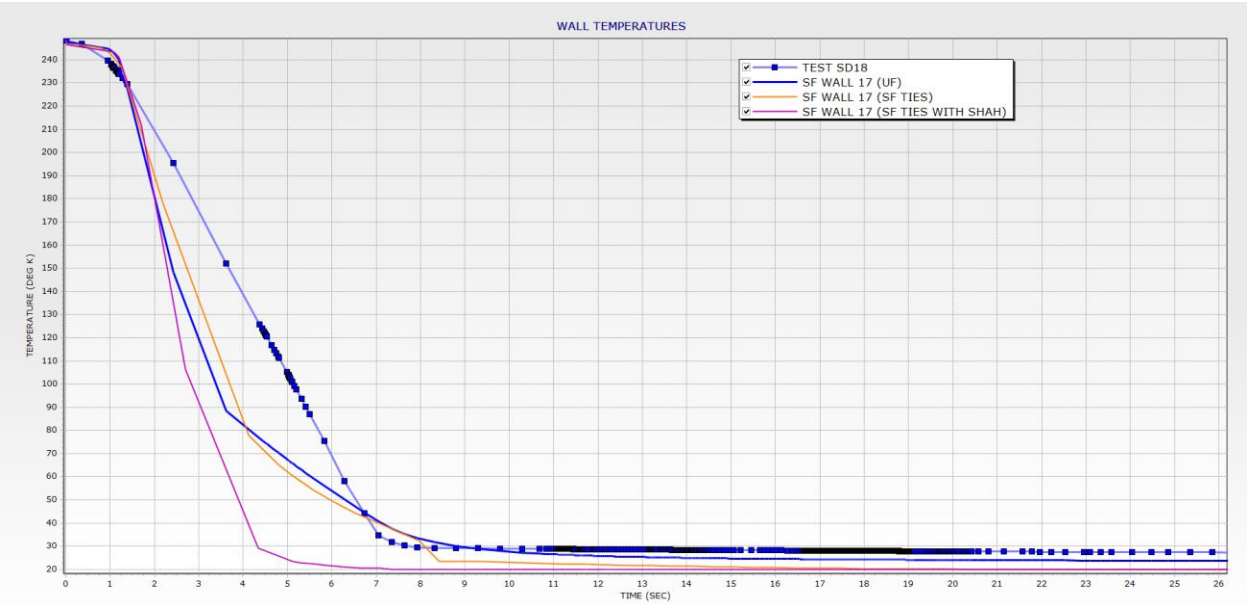

Figure 43b: Vertical Upward Liquid Hydrogen Chill-down (8b) UF and SF Heat Transfer Wall Temperature Results at Downstream Test Location (Includes Shah Modification for SF TIES)

Figure 44a: Vertical Upward Liquid Hydrogen Chill-down (8b) UF and SF Heat Transfer Void Fraction and Quality Results at Upstream Test Location (Includes Shah Modification for SF TIES)

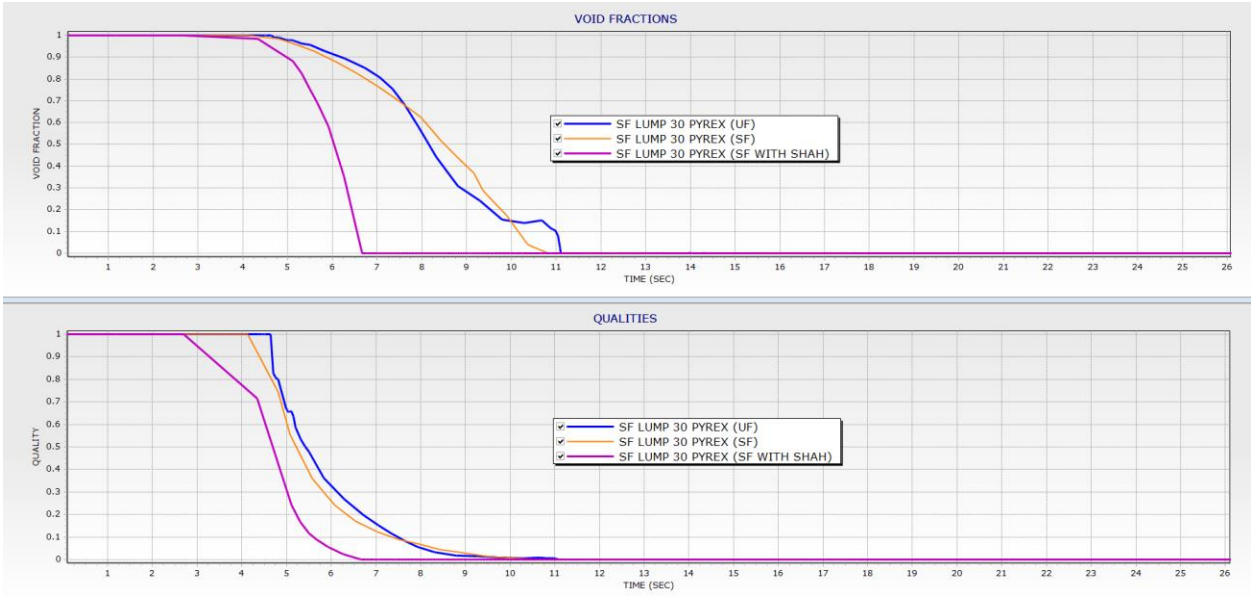

Figure 44b: Vertical Upward Liquid Hydrogen Chill-down (8b) UF and SF Heat Transfer Void Fraction and Quality Results at Sight Glass Location (Includes Shah Modification for SF TIES)

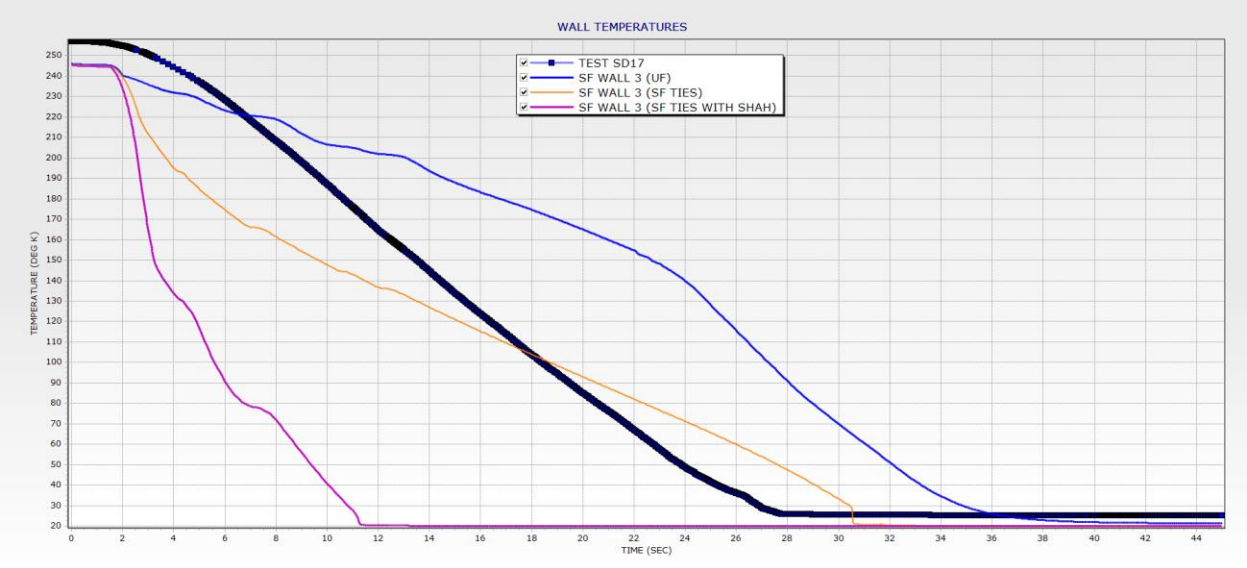

Figure 45a: Vertical Upward Liquid Hydrogen Chill-down (16b) UF and SF Heat Transfer Wall Temperature Results at Upstream Test Location (Includes Shah Modification for SF TIES)

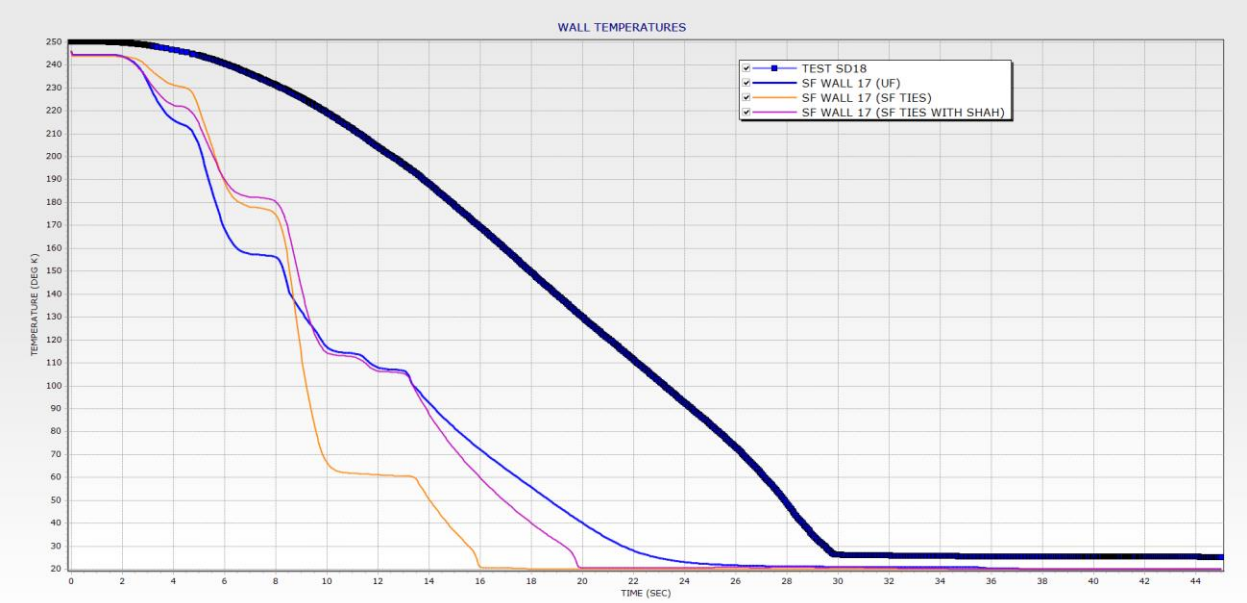

Figure 45b: Vertical Upward Liquid Hydrogen Chill-down (16b) UF and SF Heat Transfer Wall Temperature Results at Downstream Test Location (Includes Shah Modification for SF TIES)

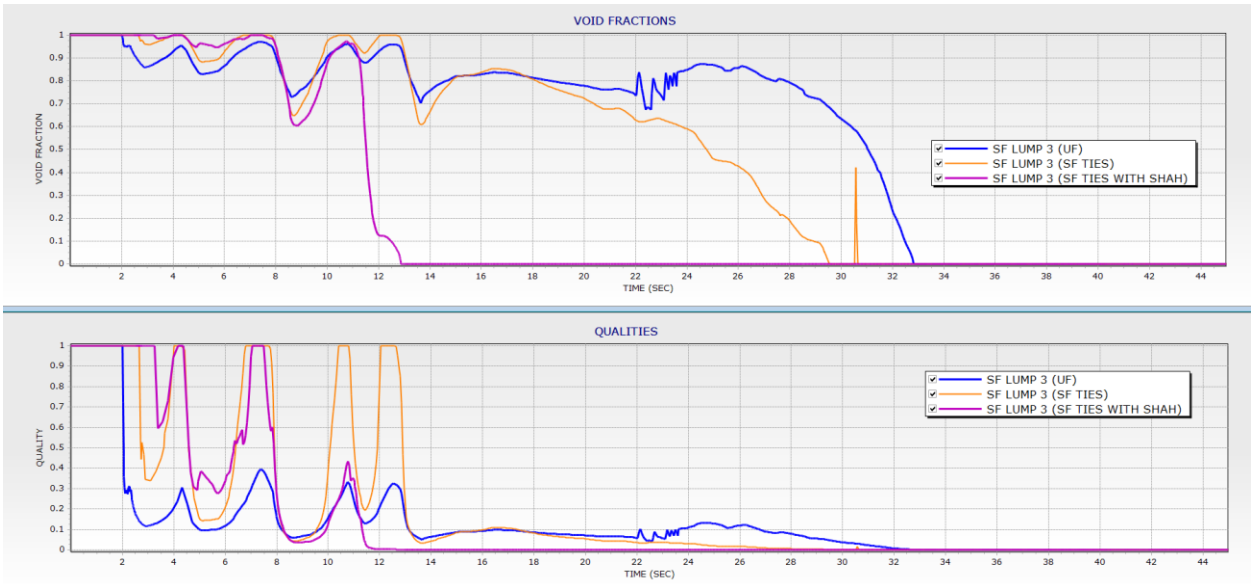

Figure 46a: Vertical Upward Liquid Hydrogen Chill-down (16b) UF and SF Heat Transfer Void Fraction and Quality Results at Upstream Test Location (Includes Shah Modification for SF TIES)

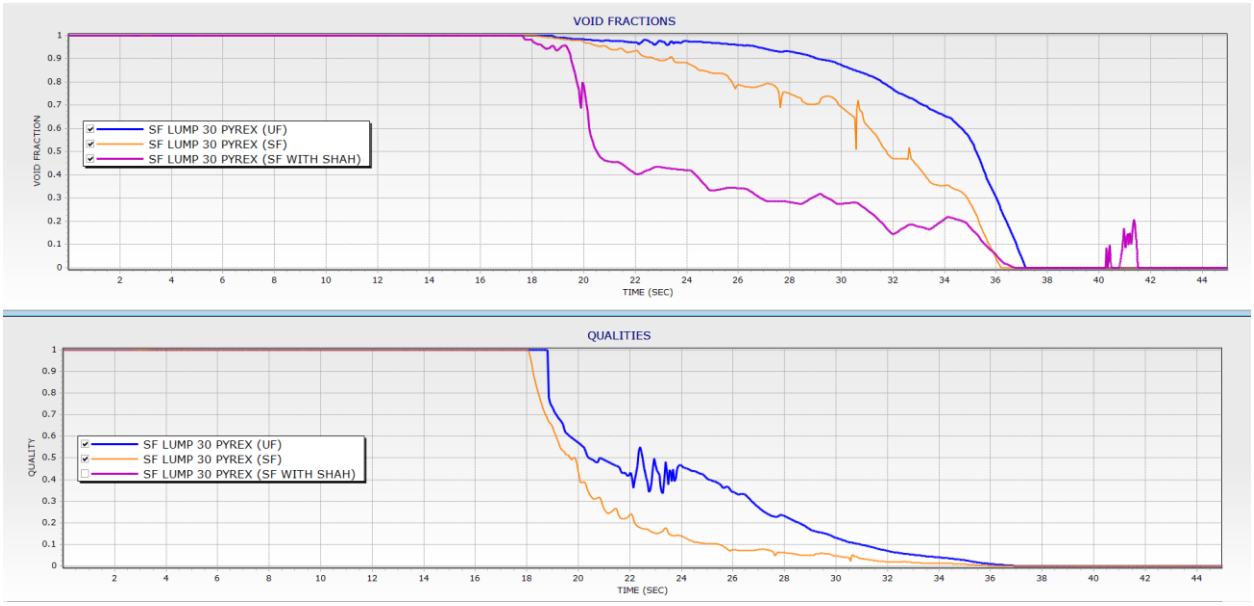

Figure 46b: Vertical Upward Liquid Hydrogen Chill-down (16b) UF and SF Heat Transfer Void Fraction and Quality Results at Sight Glass Test Location (Includes Shah Modification for SF TIES)

VII. Conclusion

In summary the University of Florida's heat transfer correlations and SINDA/FLUINT's internal correlations modelled the heat transfer in line chill down successfully except for a few cases (not necessarily the same cases) where both models yielded wall temperature results that departed from wall test data significantly. Both sets of correlations could be improved further (as demonstrated in the liquid hydrogen cases). The film boiling regime, particularly for both sets of correlations, needs improvement. University of Florida's film boiling correlation can over predict heat transfer to the wall due to flow rate oscillations. SINDA/FLUINT's correlations can either over predict or under predict the film boiling heat transfer to the wall, but is less sensitive to flow rate oscillations. In the liquid nitrogen test cases, higher Reynolds numbers seem to under predict film boiling while lower Reynolds numbers over predict

film boiling. Along with heat transfer correlations for multiphase flow, pressure drop correlations need to be addressed and/or modified since the pressure drops in all the cases did not correlate to test data, whether upstream or downstream set flow rates were employed. Also test cases with hydrogen showed that radially discretizing the wall did not significantly impact the model temperature results.

References

1. Darr, S.R., Hu, Hong, Glikin, N., Hartwig, J.W., Majumdar, A., LeClair, A., and Chung, J.N. "An Experimental Study on Terrestrial Cryogenic Transfer Line Chilldown II. Effect of Flow Direction with Respect to Gravity and New Correlation Set" *International Journal of Heat and Mass Transfer* 103, 1243 – 12460. 2016b.
2. Hartwig, J.W., McQuillen, J.B., and Rame, E. "Pulse Chilldown Tests of a Pressure Fed Liquid Hydrogen Transfer Line" *AIAA-2016-2186, AIAA SciTech Conference* San Diego, CA, January 4 – 8, 2016b.
3. Chung, J.N., "Incorporation, Integration and Evaluation of Cryogenic Transfer Line Chilldown Universal Correlations in Generalized Fluid System Simulation Program (GFSSP)" CAN NNM15AA12A, December 5, 2016.
4. Cullimore, B.A., Ring, S.G., and Johnson, D.A., Cullimore and Ring Technologies, Inc., Boulder CO, *SINDA/FLUINT General Purpose Thermal/Fluid Network Analyzer Version 5.8*, September 2015.
5. Shah, M. Mohammed, "A General Predictive Technique for Heat Transfer During Saturated Film Boiling in Tubes", *Heat Transfer Engineering*, Vol. 2, No. 2, Oct. – Dec., 1980.